State of the Global Climate 2025

WORLD METEOROLOGICAL ORGANIZATION

WMO-No. 1391

WMO-No. 1391

Chair, Publications Board
World Meteorological Organization (WMO)
7 bis, avenue de la Paix
P.O. Box 2300
CH-1211 Geneva 2, Switzerland

Tel.: +41 (0) 22 730 84 03
Email: publications@wmo.int

ISBN 978-92-63-11391-7
https://doi.org/10.59327/WMO/S/CRI/SOC1

We need your feedback

This year, the WMO team has launched a process to gather feedback on the State of the Climate reports and areas for improvement. Once you have finished reading the publication, we ask that you kindly give us your feedback by responding to this short survey. Your input is highly appreciated.

Contents

Scope

About the report

The *State of the Global Climate* is an annual WMO flagship report. It provides authoritative information on the state of the climate system by updating key observed climate indicators and presenting selected high-impact weather and climate events. It complements the work of the Intergovernmental Panel on Climate Change (IPCC) and other institutions by delivering a timely, consolidated global assessment of the year's climate conditions. The report is produced by WMO in collaboration with National Meteorological and Hydrological Services, international data centres, leading climate research institutions and United Nations partners.

What the report covers

- **Key observed global climate indicators:** global temperature, greenhouse gases, ocean heat, sea level, ocean pH, sea-ice extent, glacier mass balance and introducing a new indicator on Earth's energy imbalance.
- **High-impact weather and climate events of 2025:** heat and cold extremes, floods, droughts, tropical cyclones.
- **Case study:** climate and heat impacts on health.
- **Data sources and methods:** detailed information about the data sources and processing.

What the report does not cover

- It does not provide climate projections or forecasts.
- It does not provide in-depth scientific discussion.
- It does not provide extensive regional or national detail.
- It does not prescribe policy actions or mitigation pathways.

Who this report is for

- **National Hydrological and Meteorological Services**, to provide global context to regional and national climate information.
- **Policymakers**, to inform global, regional and national climate decisions.
- **Scientists and technical experts**, as a reference for climate data and trends of key climate indicators.
- **Media and educators**, for an accurate and accessible synthesis of climate information.
- **General public and youth**, to better understand how the climate is changing.

Other relevant WMO reports

- Regional *State of the Climate* reports for Africa, Asia, Latin America and the Caribbean, South-West Pacific and Europe (with the Copernicus Climate Change Service (C3S)) provide more detailed regional analyses of key climate indicators alongside impact and risk information.
- The ***State of Global Water Resources*** is a comprehensive quantitative overview of global water resources, with a focus on hydrological variability and trends.
- The ***WMO Greenhouse Gas Bulletin*** is an update of the status of key greenhouse gases in the atmosphere.
- WMO El Niño/La Niña Updates are regular reports on the state and forecasts for the El Niño Southern Oscillation.

How to cite

World Meteorological Organization (WMO). *State of the Global Climate 2025*. (WMO-No. 1342). Geneva, 2026. ISBN: 978-92-63-11299-7.
https://doi.org/10.59327/WMO/S/CRI/SOC1

Summary

The temperature of the Earth changes in response to the rate at which energy enters and leaves the Earth system. Increasing concentrations of greenhouse gases in the atmosphere such as **carbon dioxide**, methane and nitrous oxide, all of which reached their highest level in 800 000 years in 2024 (the last year for which we have consolidated global figures), reduce the rate at which energy leaves the Earth system. This imbalance – the **Earth's energy imbalance**, a new indicator in this year's report – leads to an accumulation of excess energy.

One of the longest observational records of climate change is that of **global mean near-surface temperature**. The past three years are the three warmest years in the 176-year combined land and ocean observational record. The year 2025 is the second or third warmest year, depending on the dataset used, slightly cooler than the record warmth of 2024, due in part to the **transition from El Niño at the start of 2024 to La Niña** in 2025. The warming seen at the surface and throughout the troposphere represents just 1% of the excess energy trapped by greenhouse gases.

The vast majority of the excess energy – around 91% – has been absorbed by the ocean in the form of heat. **Ocean heat content** reached a new record high in 2025, reflecting the continued increase in energy.

Another 3% of the excess energy warms and melts ice. In a **global set of reference glaciers** with long-term measurements, eight of the ten most negative annual glacier mass balances since 1950 have occurred since 2016. The ice sheets on Antarctica and Greenland have both lost significant mass since satellite records began.

The **extent of sea ice in the Arctic** has decreased in all seasons since satellite measurements began in 1979, and the annual maximum extent in 2025 was the lowest or second lowest in the observed records. **Sea-ice extent around Antarctica** showed a small long-term increase until 2015, but since then, extents throughout the annual cycle have dropped considerably, and the past four years have seen the four lowest Antarctic sea-ice minima on record.

The warming ocean and melting of ice on land from glaciers and ice sheets have both contributed to the long-term rise in **global mean sea level**. The rate of global sea-level rise has increased since satellite measurements began in 1993.

The remaining ~5% of the excess energy is stored in the continents, increasing the temperature of the land mass and thereby affecting terrestrial processes.

As well as absorbing the majority of the energy trapped by increasing concentrations of greenhouse gases, the ocean has also absorbed around 29% of the anthropogenic emissions of carbon dioxide in the past decade. While this helps to buffer the effects of climate change, it also alters the chemical composition of the ocean water, **reducing the pH in a process known as ocean acidification**.

These rapid large-scale changes in the Earth system have cascading impacts on human and natural systems, contributing to food insecurity and displacement where hazards intersect with high vulnerability and limited adaptive capacity.

KEY INDICATOR

Atmospheric carbon dioxide

Key messages

In 2024, the atmospheric concentration of carbon dioxide reached its highest level in the last 2 million years. Levels of methane and nitrous oxide reached their highest levels in the last 800 000 years.

The increase in the annual carbon dioxide concentration in 2024 was the largest annual increase since modern measurements began in 1957.

Real-time data from individual locations show that levels of these three main greenhouse gases continued to increase in 2025.

State of the indicator

The global annual average mole fraction of carbon dioxide (CO_2) in the atmosphere — the atmospheric concentration — reached a new observed high in 2024, the latest year for which consolidated global figures are available (Figure 1). At 423.9 ± 0.2 parts per million (ppm), the concentration in 2024 was 3.5 ppm more than in 2023 and 152% of the estimated pre-industrial concentration (in 1750).[1] The concentration of 423.9 ppm corresponds to about 3 306 Gt CO_2 in the atmosphere.

The increase in 2024 was the largest annual increase in the CO_2 concentration since modern measurements began in 1957. This increase was driven by continued fossil CO_2 emissions, increased fire emissions and reduced effectiveness of terrestrial and ocean sinks in 2024. Concentrations of methane (CH_4) and nitrous oxide (N_2O), two other key greenhouse gases, also reached record high observed levels in 2024. The concentration of CH_4 reached 1 942 ± 2 parts per billion (ppb), 266% of pre-industrial levels, and that of N_2O reached 338.0 ± 0.1 ppb, 125% of pre-industrial levels.

Real-time data from individual stations show that levels of CO_2, CH_4 and N_2O continued to increase in 2025.

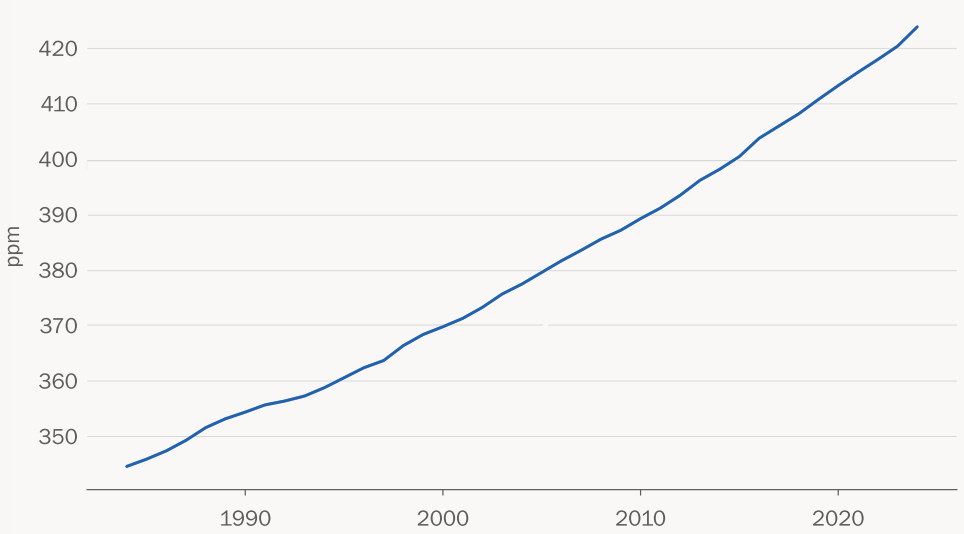

Figure 1. Annual mean globally averaged atmospheric mole fraction of carbon dioxide from 1984 to 2024 in parts per million (ppm)
Source: Data are from the World Data Centre for Greenhouse Gases (WDCGG). See Datasets and methods.

Indicator background

The human-caused increase in the concentration of CO_2 in the atmosphere is the largest driver of climate change. CO_2 accounts for around 66% of the radiative forcing by all long-lived greenhouse gases since 1750 and about 79% of the increase over the past decade.[2] Current atmospheric concentrations of CO_2 are higher than at any time in at least 2 million years[3] based on proxy data. Concentrations of CH_4 and N_2O are higher than at any time in at least 800 000 years.

The concentrations of greenhouse gases presented here (Figure 1) are estimated from measurements made across a globally coordinated network covering the period 1984-2024. Pre-industrial concentrations are estimated using air trapped in ice cores with the year 1750 being used to represent pre-industrial conditions.

Atmospheric concentrations of CO_2 reflect a balance between CO_2 sources and sinks. The anthropogenic sources of CO_2 are related to the burning of fossil fuel and cement production along with land use changes such as deforestation. Sinks of CO_2 include uptake by vegetation and the ocean.

The portion of CO_2 emitted by human activities that remains in the atmosphere is known as the airborne fraction. It varies from year to year due to the high natural variability of CO_2 sinks, particularly those on land. Natural sources and sinks of CO_2 are affected by climate change via increasing temperature, changes in precipitation, and susceptibility to biomass burning.

During the 2015–2024 period, 50% of the total emissions of CO_2 remained in the atmosphere, driving the increase in atmospheric concentrations. The estimated ocean sink accounted for 29% of emissions and the estimated land sink accounted for 21%.[4]

Associated risks of atmospheric CO_2 and the Sustainable Development Goals

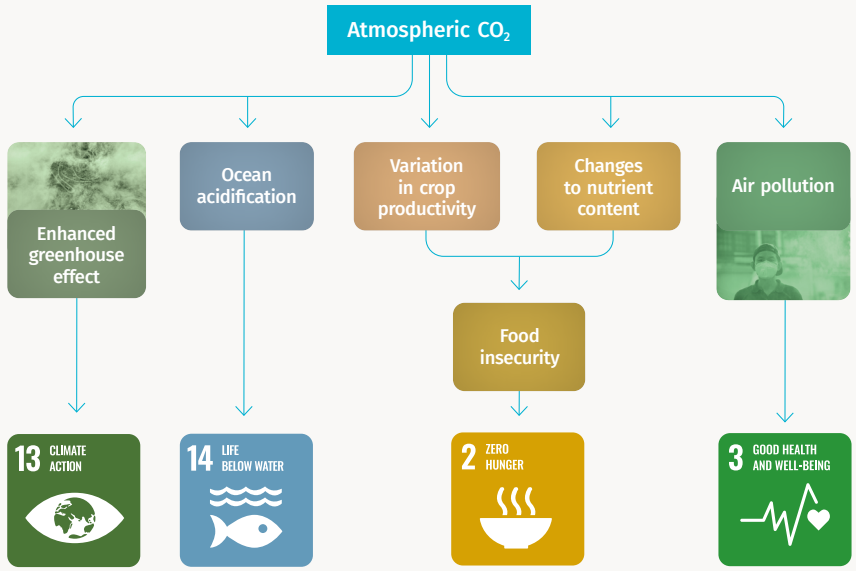

KEY INDICATOR

Global mean near-surface temperature

Key messages

The annually averaged global mean near-surface temperature in 2025 was 1.43 °C ± 0.13 °C above the 1850–1900 average used to represent pre-industrial conditions.

The year 2025 was the second or third warmest year in the 176-year observational record, depending on which of nine datasets is used. The year 2024 remains the warmest year in all the datasets, at 1.55 °C ± 0.13 °C above the 1850–1900 average.

For global mean temperature, the past eleven years, 2015–2025, were the eleven warmest years on record.

State of the indicator

Based on a synthesis of nine global temperature datasets (see Datasets and methods), the annually averaged global mean near-surface temperature in 2025 was 1.43 °C ± 0.13 °C (90% uncertainty range) above the 1850–1900 average. Depending on the dataset used, 2025 was the second (two datasets) or third (seven datasets) warmest in the 176-year observational record (Figure 2). The warmest year was 2024 with an anomaly of 1.55 °C ± 0.13 °C. The past eleven years, 2015-2025, were the eleven warmest years on record and the past three years 2023–2025, the three warmest in all nine datasets.

The annual global mean temperature of 2025 was lower than the record high of 2024, consistent with the shift from a strong El Niño at the start of 2024 to weak La Niña conditions at the start and end of 2025. Despite this, 2025 continued a run of exceptionally high global temperatures and January 2025 was the warmest January on record.

In 2025, the global mean land temperature was the second or third highest on record at 0.80 °C above the 1991–2020 average. The global mean sea-surface temperature (SST) – the temperature in the upper few metres of the ocean – was the third highest on record at 0.39 °C above the 1991–2020 average. Despite La Niña conditions, around 90% of the ocean surface area experienced at least one marine heatwave during 2025 and only 18% experienced a marine cold wave. Ocean heat content, referring to the upper 2 000 metres of the ocean, was the highest on record (see Ocean heat content). SST is more variable than ocean heat content because it represents the temperature of a much thinner layer (a few metres for SST as compared to 2 000 m for ocean heat content) which can thus change temperature more quickly.

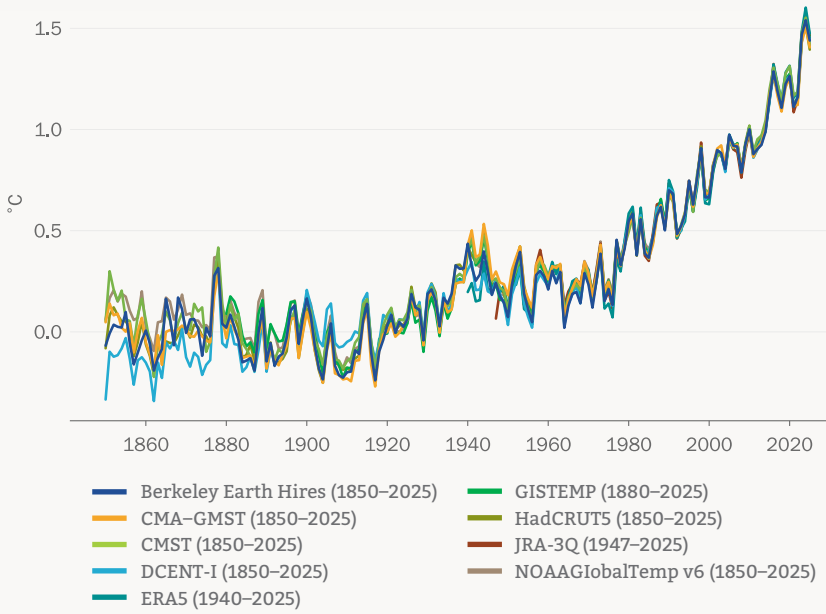

Figure 2. Annual global mean temperature anomalies relative to a pre-industrial (1850–1900) baseline shown from 1850 to 2025

Source: Data are from the datasets indicated in the legend. For details see Datasets and methods.

Indicator background

Global mean near-surface temperature is the temperature near the surface of the Earth averaged across its whole surface. Global mean temperature is estimated using air temperatures measured at weather stations at a height of around 1.5 to 2 m and sea-surface temperatures measured by ships and ocean buoys. Data are quality controlled and corrected for changes in how temperatures were measured, then gaps are filled using statistical methods. Global mean temperature can also be calculated using reanalyses, which use a weather forecasting system to combine many kinds of measurement, including satellite measurements, into globally complete fields. Reanalysis-based estimates are representative of air temperature across land and ocean.

Nine datasets, including two reanalyses, were used to assess global temperature in this report (see **Datasets and methods**). Together they cover the period from 1850 to the present, though not every dataset covers the whole period from 1850 (see Figure 2). There are minor differences between the series, however they show largely the same variations during the period in which they overlap. Differences are larger earlier in the record, leading to small differences in their assessment of long-term change (around 0.1 °C–0.2 °C). These differences are factored into the uncertainty estimates for anomalies relative to 1850–1900.

A single year with an annual global mean temperature over 1.5 °C above the 1850–1900 average, such as 2024, does not indicate that we have exceeded the 1.5 °C warming level mentioned in the long-term temperature goal of the Paris Agreement, because the goal refers to changes over decades not individual years.

Associated risks of increased global mean surface temperature and the Sustainable Development Goals

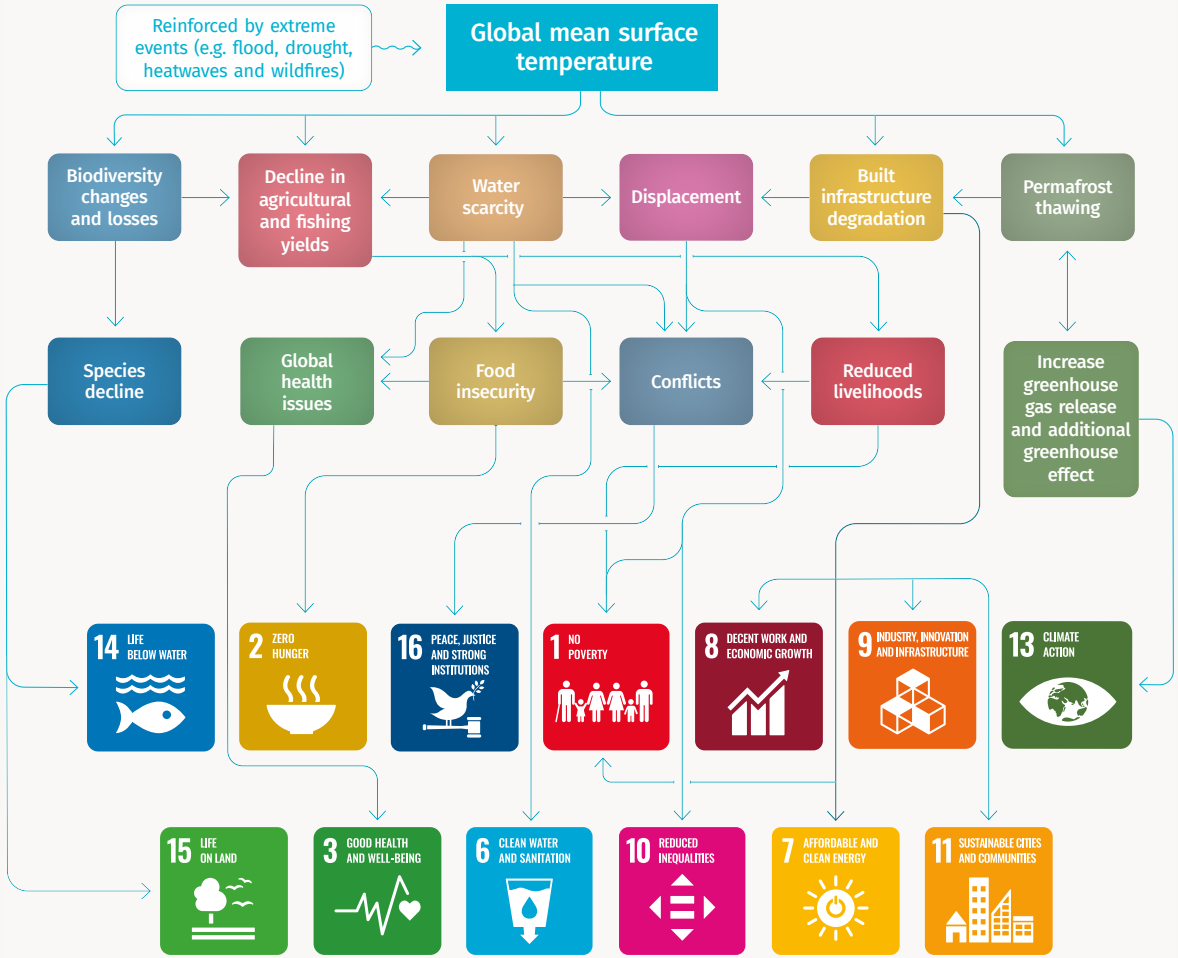

KEY INDICATOR

Ocean heat content

Key messages

In 2025, ocean heat content reached the highest level in the 66-year observational record, exceeding the previous record high set in 2024.

Over the past nine years, each year has set a new record for ocean heat content.

The rate of ocean warming over the past two decades, 2005–2025, is more than twice that observed over the period 1960–2005.

State of the indicator

In 2025, observed global ocean heat content (in the upper 2 000 m of the ocean) set a record,[5] exceeding the previous record set in 2024 by 24 ± 16 ZJ (Figure 3). Over the past nine years, each year has set a new record for ocean heat content. Instrumental records of global ocean heat content start around 1960.

The rate of ocean warming over the past two decades (2005–2025) was 11.0–12.2 ZJ per year, which is more than twice that observed over the period 1960–2005, for which the rate was 3.05–3.91 ZJ per year.

The latest Intergovernmental Panel on Climate Change (IPCC) report concluded that it was virtually certain that ocean heat content had increased since the 1970s and extremely likely that the main driver was human influence. Based on the datasets used here, global ocean heat content increased at a rate of 5.8 ± 0.5 ZJ per year averaged over the area of the ocean from 1971 to 2025, which is consistent with the IPCC report.[6] Over the period 1970–2025, the deep ocean (2 000–6 000 m) warmed at a rate of 1 ± 0.2 ZJ per year.[7]

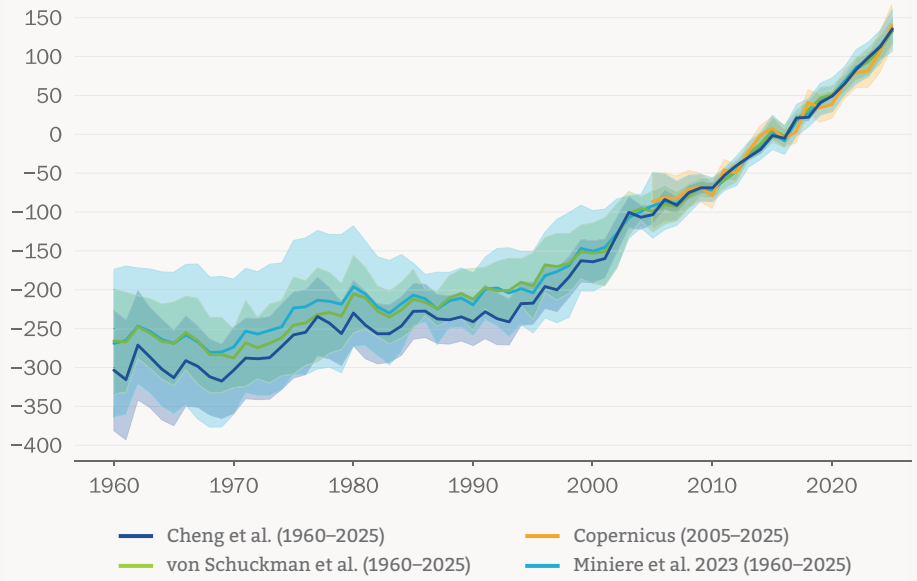

Figure 3. Annual global ocean heat content down to 2 000 m depth for the period 1960–2025, in zettajoules (ZJ). One zettajoule is 10^{21} joules. The shaded area indicates the 2-sigma uncertainty range on each estimate. For details see Datasets and methods.

Indicator background

The rate of ocean warming reveals how rapidly the Earth system is trapping surplus energy in the form of heat from climate forcings. Around 5% of that surplus energy is warming the land, 1% is warming the atmosphere and 3% is warming and melting the cryosphere. However, the majority, around 91%, goes into warming the ocean.[8] Changes in ocean heat content are therefore a key indicator of climate change.

The integration of ocean temperatures from the surface to a depth of 2 000 m provides a measure of ocean heat content.[9, 10] Ocean temperatures have been measured by research ships for over a century, but observations are too sparse to form a global average before around 1960 and, for the ocean below 2 000 m, before around 1970. Additional measurements have been made using expendable devices launched from ships since the 1970s and, since around 2005, near-global coverage down to 2 000 m has been provided by autonomous Argo buoys.

Changes in global ocean temperature are irreversible on centennial to millennial timescales. Climate projections show that ocean warming will continue over the twenty-first century and beyond as a result of the existing energy imbalance in the Earth system, even if future emissions are significantly reduced.[11]

Ocean warming has wide-reaching consequences, such as degradation of marine ecosystems, biodiversity loss and reduction of the ocean carbon sink. It fuels tropical and subtropical storms and exacerbates ongoing sea-ice loss in the polar regions. Ocean warming together with ice loss on land is driving sea-level rise.[12]

Associated risks of increased ocean heat content and the Sustainable Development Goals

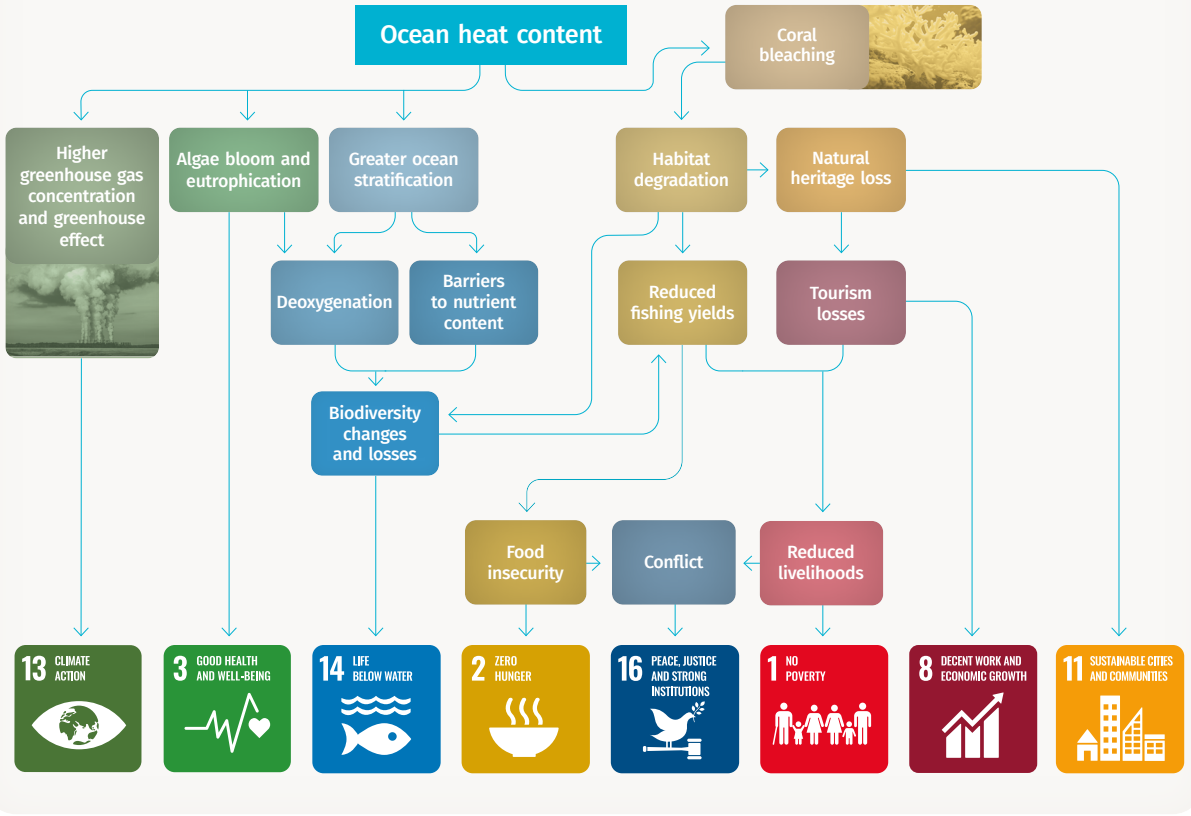

KEY INDICATOR

Global mean sea level

Key messages

In 2025, global mean sea level was comparable to the record-high levels observed in 2024 in the satellite altimetry record.

The year-to-year increase from 2024 to 2025 was smaller than 2023 to 2024, consistent with short-term variability associated with La Niña conditions.

The rate of global mean sea-level rise since 2012 is higher than the rate of global mean sea-level rise in the earlier part of the satellite record, 1993–2011.

State of the indicator

Satellite altimetry records showed a rapid increase in global mean sea level of about 5 mm over 2023 and 2024 (Figure 4) associated with a strong El Niño that ended in early 2024.[13] In 2025, global mean sea level continued at levels comparable to 2024, reflecting the transition from El Niño to weak La Niña conditions (see **Climate driver: El Niño–Southern Oscillation**). The year-to-year increase from 2024 to 2025 was therefore smaller than from 2023 to 2024.

At the end of 2025, the global mean sea level was around 11 cm higher than it was in January 1993, the start of the satellite record. The mean rate of sea-level rise has increased with time. From 1993 to 2011, sea level rose at an average rate of 2.65 ± 0.3 mm per year. During the period 2012 to 2025, the rate was 4.75 ± 0.3 mm year.[14]

Sea level has risen since 1993 in all oceanic regions, except for an area of the Southern Ocean in the Pacific sector. Some areas have risen faster than the global mean, including the tropical and south-western Pacific, as well as north of 30°N in the Pacific. Areas where sea-level rise was slower than the global mean include the eastern Pacific, south Indian Ocean and north Atlantic south of Greenland. The rate of sea-level rise over the past 33 years in the Indian Ocean, north of 30°S, and in the tropical and eastern Atlantic Ocean, has been similar to the global mean.

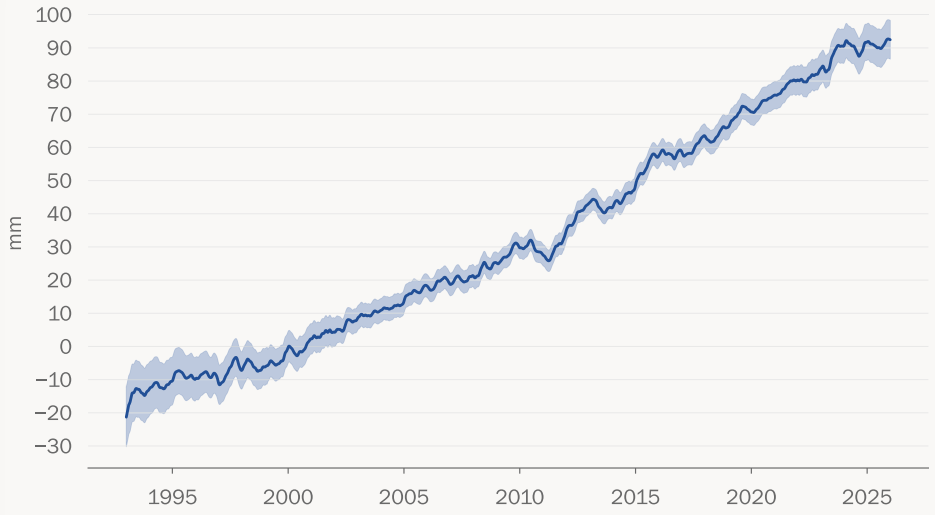

Figure 4. Global mean sea level change (change from January 1993 in mm) shown for 1993–2025. The seasonal cycle has been removed from the data. The shaded area indicates the uncertainty.

Source: Data from Aviso, Centre national d'études spatiales (CNES). For details see Datasets and methods.

Indicator background

Global mean sea level is measured by satellites using radar altimeters that record the time taken for a radar signal to reach the sea surface and return to the satellite. Longer records of global mean sea level exist based on tide gauge measurements made along coastlines around the world since the late nineteenth century. While satellites provide near-global coverage, tide gauges provide ground truth data used to calibrate and validate the satellite-based estimates.

The warming of the ocean causes the water to expand and global mean sea level to rise. The melting of ice on the land also contributes to sea-level rise. Because warming of the oceans will continue for centuries even if emissions of greenhouse gases cease, sea level will continue to rise on the same timescale.

Changes in sea level have wide-ranging effects on coastal areas and communities. Sea-level rise will bring cascading and compounding impacts,[15] resulting in losses of coastal ecosystems and ecosystem services, groundwater salinization, flooding and damage to coastal infrastructure. These impacts cascade into risks to livelihoods, settlements, health, well-being, food and water security, as well as cultural values in the near to long term.

Associated risks of increased sea-level rise and the Sustainable Development Goals

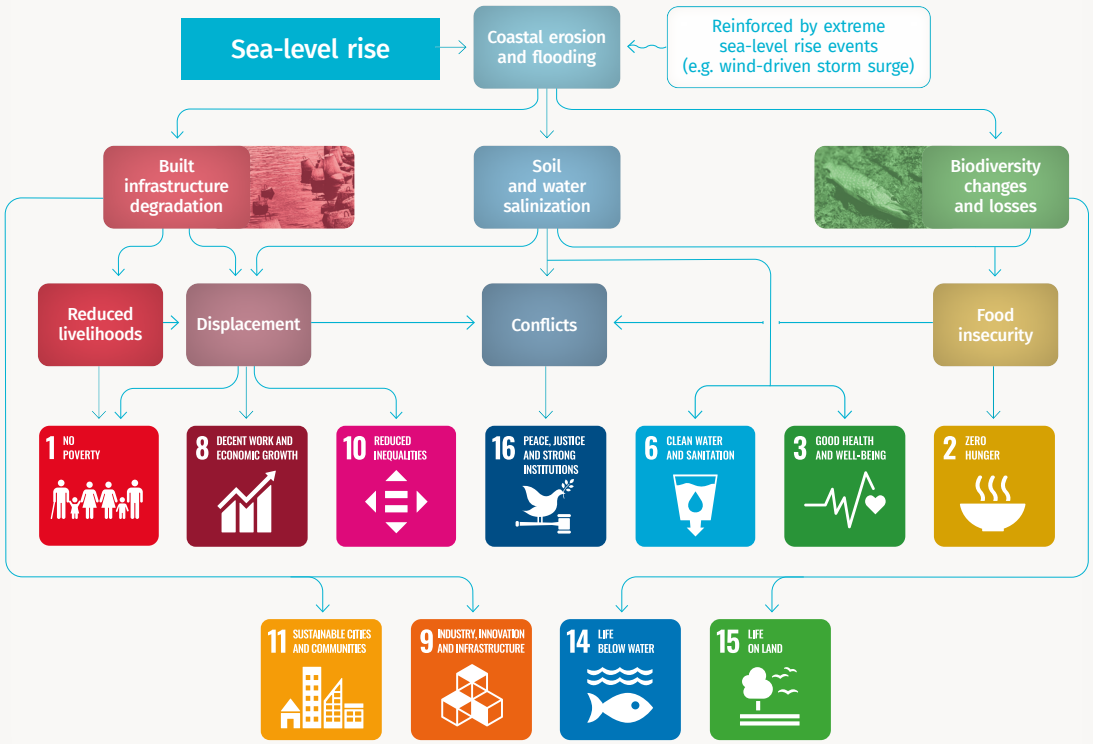

KEY INDICATOR

Ocean pH

Key messages

Global average ocean surface pH has declined over the past 41 years.

Ocean surface pH is not changing uniformly across regions.

State of the indicator

Globally, ocean surface pH has changed at a rate of –0.017 ± 0.001 pH units per decade over the period 1985–2025 (Figure 5). The rate of change in pH is consistent with the observation-based estimates of the latest IPCC report which concluded "*it is virtually certain* that surface open ocean pH has declined globally over the last 40 years by 0.003–0.026 pH per decade".[16]

Regionally, changes in surface ocean pH have not proceeded uniformly. The largest decreases in regional surface pH are observed in the Indian Ocean, the Southern Ocean, the eastern equatorial Pacific Ocean, the northern tropical Pacific and some regions in the Atlantic Ocean. In these areas, which amount to 47% of the sampled global ocean, the surface of the ocean is getting more acidic at a faster rate than the global average.[17]

Indicator background

Around 29% of the CO_2 emitted by human activities during the decade 2015–2024 was absorbed by the ocean.[18] This process has caused a shift in the carbonate chemistry of the ocean, leading to a drop in pH. While the ocean surface pH at above 7 is still alkaline, these changes are acidifying the ocean. The Sixth Assessment Report (AR6) of the Intergovernmental Panel on Climate Change (IPCC) concluded that "[t]here is very high confidence that present-day surface pH values are unprecedented for at least 26,000 years and current rates of pH change are unprecedented since at least that time".[19]

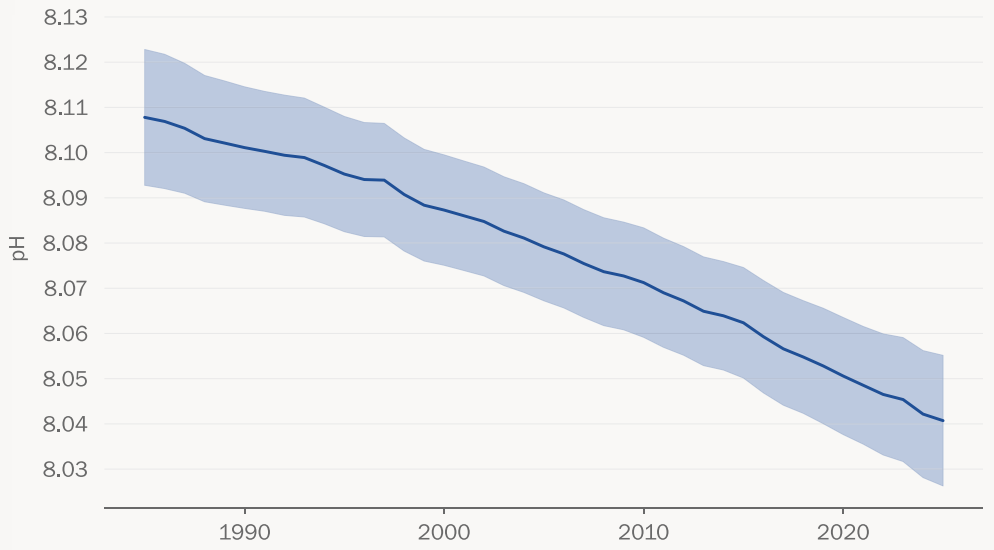

Figure 5. Annual global mean surface ocean pH 1985 to 2025. The dark line is the central estimate, and the shaded area is the uncertainty range.

Source: Data from Copernicus Marine Environment Monitoring Service (CMEMS). For details see Datasets and methods.

Surface ocean pH is monitored through sustained global carbon observations compiled since the mid-1980s and integrated into global reconstructions.[20] These provide a consistent and comparable historical record of change that is used here as an indicator. CO_2 absorbed at the ocean surface is transported into the ocean interior by ocean currents and mixing,[21] contributing to acidification at depth. While acidification extends into the ocean interior, carbonate chemistry observations at depth remain more limited. Based on the available evidence, the IPCC concluded that "[o]ver the past 2–3 decades, a pH decline in the ocean interior has been observed in all ocean basins (*high confidence*)."[22]

Climate projections show that ocean pH will continue to decrease in the twenty-first century, at rates dependent on future emissions. Changes in deep-ocean pH are irreversible on centennial to millennial timescales.[23]

It is well established that ocean acidification is affecting marine life across ocean depths. The responses of marine organisms to the compound effects of acidification, ocean warming and deoxygenation occur at different metabolic levels for different groups, and include respiratory stress and reduction of thermal tolerance.[24]

The effects of ocean acidification on habitat area, biodiversity, ecosystem function and ecosystem services have already been clearly observed, and food production from shellfish aquaculture and fisheries has been adversely affected.[25]

Warm-water coral reefs and rocky shores dominated by immobile, calcifying organisms that produce shells and skeletons, such as corals, barnacles and mussels, are also affected by extreme temperatures and changes in pH.[26] The monitoring of surface ocean pH has become a focus of many international scientific initiatives and constitutes one target for **Sustainable Development Goal (SDG) 14: Conserve and sustainably use the oceans, seas and marine resources for sustainable development**.

Associated risks of increased ocean acidification and the Sustainable Development Goals

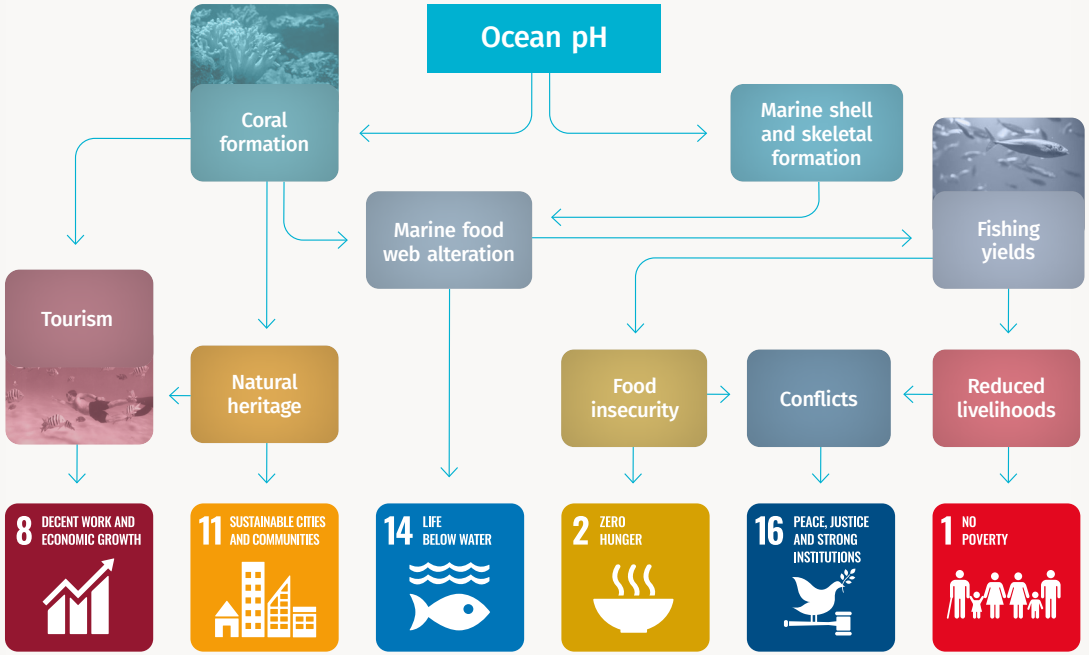

KEY INDICATOR

Glacier mass balance

Key messages

In the 2024/2025 hydrological year (September 2024–August 2025), glacier mass loss from a set of reference glaciers was among the five most negative glacier mass balances on record. Eight of the ten most negative annual glacier mass balances since 1950 have occurred since 2016.

In 2025, exceptional levels of glacier mass loss occurred in Iceland, and along the Pacific coast of North America.

State of the indicator

Data on glacier mass balance – the amount of mass gained or lost by glaciers – for the 2024/2025 hydrological year (September–August) are not yet finalized, but observations from 155 of the ~170 glaciers that are reported annually to the World Glacier Monitoring Service indicate that 2024/2025 was another year of extremely negative mass balance worldwide (Figure 6).

Exceptionally negative mass balances were recorded in Iceland (which had its warmest year on record) and along the Pacific coast of North America.

Overall mass balance in 2024/2025 as estimated from a set of reference glaciers was among the five lowest glacier mass balances on record (1950-2025) and less negative than the record loss in 2022/2023. The 2024/2025 mass balance was close to the average for the preceding three years, 2021/2022 to 2023/2024, which saw the largest negative three-year mass balance on record. This continues a trend of accelerated glacier mass loss in recent years: 8 of the 10 largest negative mass balance years since 1950 have occurred since 2016.

Indicator background

Glaciers are formed from snow that has compacted to form ice, which then deforms and flows downhill. Glaciers comprise two zones: an accumulation zone where accumulation of mass from snowfall exceeds ice loss, and an ablation zone where ice loss (ablation) from melting and other mechanisms exceeds accumulation. Where glaciers end in a lake or the ocean, ice loss can occur

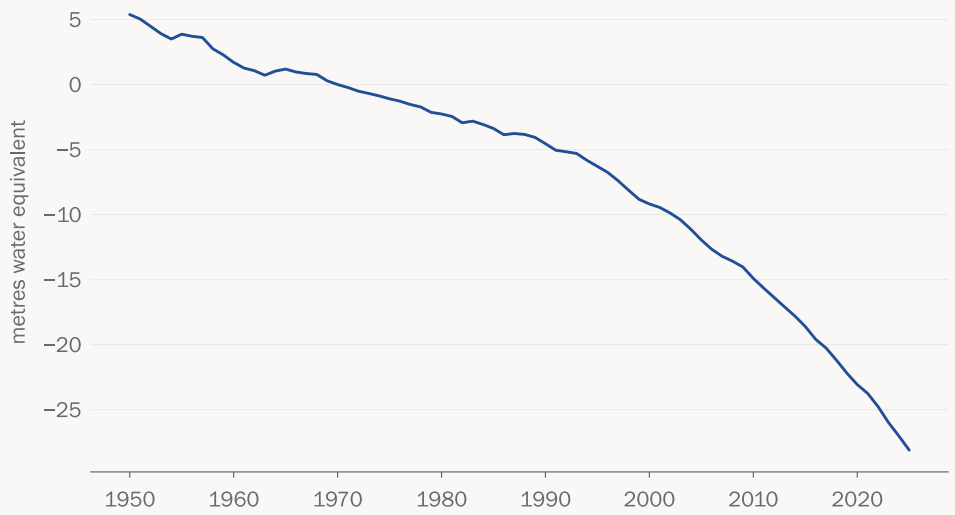

Figure 6. Cumulative annual mass balance (change since 1970) of reference glaciers with more than 30 years of ongoing glaciological measurements. Annual mass change values are expressed in metres water equivalent, which corresponds to tonnes per square metre (1 000 kg m^{-2}).

Source: World Glacier Monitoring Service. For details see Datasets and methods.

through melting where the ice meets the water, and via calving when chunks of the glacier break off.

Glacier mass balance – the amount of mass gained or lost by the glacier – is commonly expressed as the annual thickness change averaged over the glacier area, expressed in metres water equivalent. One metre water equivalent is approximately the same as one tonne per square metre. Ice loss from glaciers contributed around 21% of the total sea-level rise over the period 1993–2018. By way of comparison, ocean warming contributed 42% of the total rise, and melting of the ice sheets in Greenland and Antarctica contributed 15% and 8% respectively.[27]

The mass balances of individual glaciers are affected by changes in temperature, precipitation, humidity and cloudiness. Variability in these can lead to positive mass balance in some years even where the mass balance is negative over the long term. The IPCC Sixth Assessment Report (AR6) concluded that human influence is very likely the main driver of the global retreat of glaciers since the 1990s, stating that "[t]he global nature of glacier retreat since the 1950s, with almost all of the world's glaciers retreating synchronously, is unprecedented in at least the last 2 000 years (medium confidence)".[28]

Melt rates are also strongly affected by the glacier albedo, the fraction of sunlight that is reflected by the glacier surface. Exposed glacier ice is darker and therefore has a lower albedo than the seasonal snowpack; it is also sensitive to darkening from mineral dust, black carbon, algal activity and fallout from forest fires. Reduced snow cover, long melt seasons and wildfire activity all concentrate darker material on the glacier surface, decreasing its albedo and thereby increasing the rate of melting.

Associated risks of declining glacial mass balance and the Sustainable Development Goals

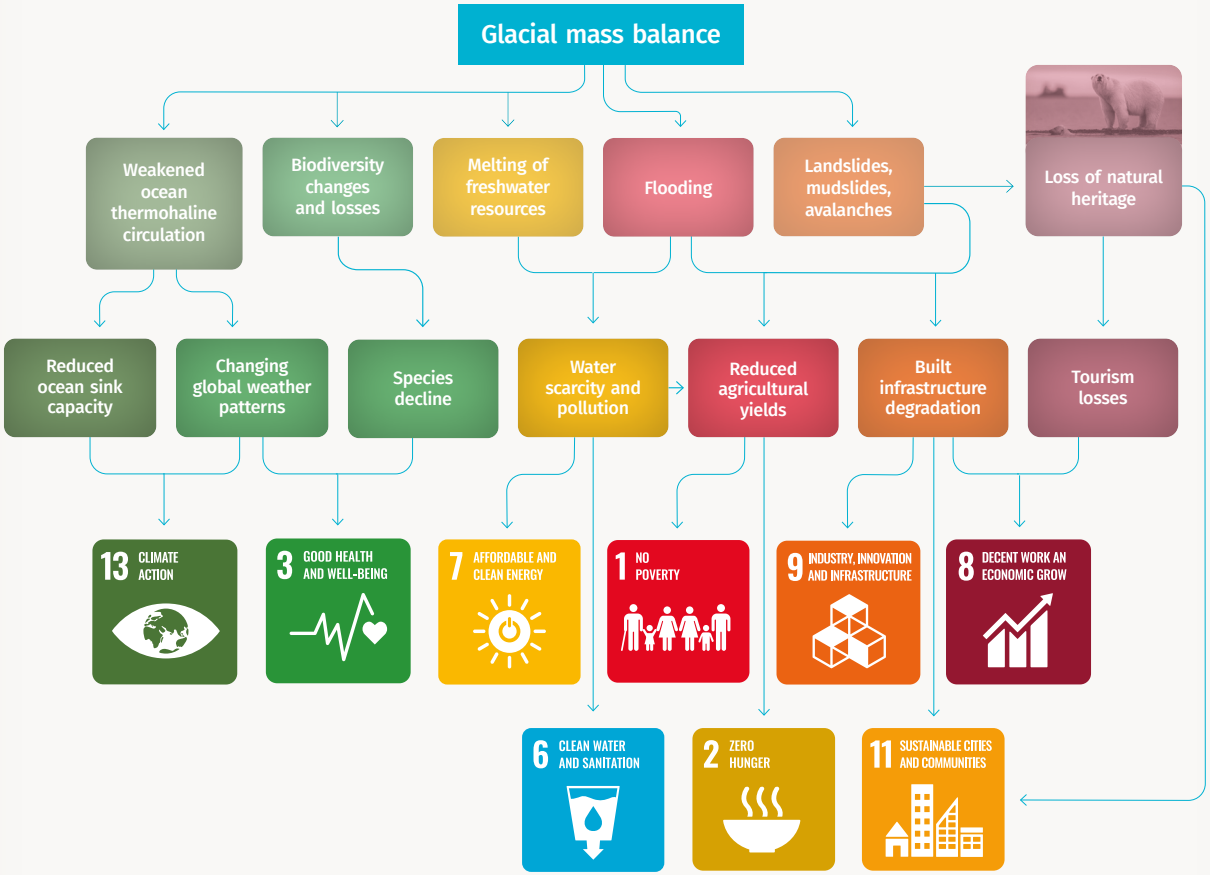

KEY INDICATOR

Sea-ice extent

Key messages

The annual average Arctic sea-ice extent for 2025 was the lowest or second lowest on record in the satellite era, and the average Antarctic sea-ice extent for 2025 was the third lowest after 2023 and 2024.

The maximum daily extent of Arctic sea-ice in 2025 was the lowest annual maximum in the observed record (1979 to present) at 14.19 ± 0.40 million km² between 20 and 21 March.

The annual minimum daily extent of Antarctic sea-ice tied for the second lowest in the observed record (1979 to present).

State of the indicator

The extent of sea-ice in the Antarctic and Arctic regions in 2025 were both below their respective 1991–2020 averages throughout the annual cycle (Figure 7).

Annual average Arctic sea-ice extent in 2025 was the lowest or second lowest in the satellite era (1979 to present) at 10.10 ± 0.33 million km² (see Datasets and methods) compared to the long-term average of 11.01 ± 0.29 million km². The extent in 2020 was similar.

Following a delayed freeze in 2024, Arctic sea-ice saw its lowest maximum extent on record in 2025, peaking at 14.19 ± 0.40 million km² on 20 or 21 March, compared with the average annual maximum of 15.07 ± 0.38 million km². The annual minimum extent of 4.74 ± 0.35 million km² on 7 or 8 September was between the tenth and fourteenth lowest extent on record, and 0.73 million km² below average. As in 2024, freeze-up was delayed in late 2025, and the December extent was the lowest on record for December.

Annual average Antarctic ice extent in 2025 was the third lowest since 1979 at 10.81 ± 0.26 million km², higher only than in 2023 and 2024.

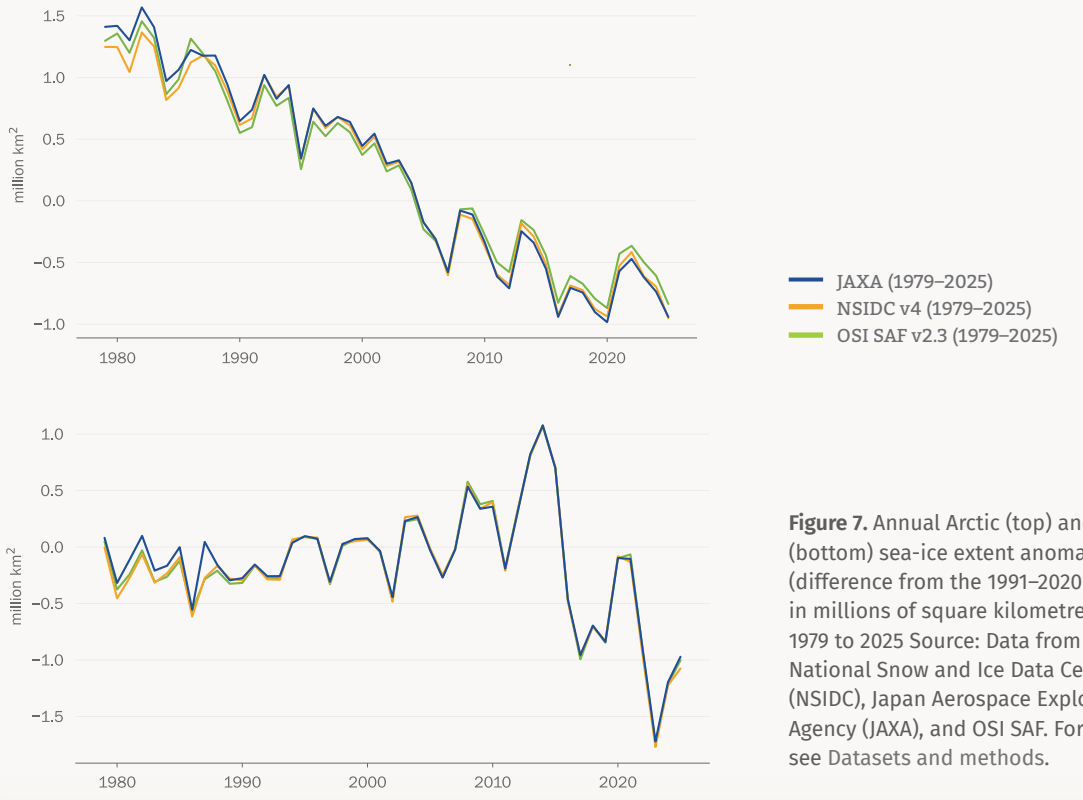

Figure 7. Annual Arctic (top) and Antarctic (bottom) sea-ice extent anomalies (difference from the 1991–2020 average) in millions of square kilometres from 1979 to 2025 Source: Data from the USA National Snow and Ice Data Center (NSIDC), Japan Aerospace Exploration Agency (JAXA), and OSI SAF. For details see Datasets and methods.

Antarctic sea-ice extent reached a minimum of 2.06 ± 0.10 million km^2 between 23 February and 1 March 2025, tied for the second lowest minimum on record. The past four years have seen the four lowest Antarctic ice minima on record, far below the average minimum of 2.93 ± 0.14 million km^2. Antarctic sea-ice cover reached its annual maximum extent of 18 ± 0.28 million km^2 around 15 September 2025, around 1 million km^2 below the average maximum.

Indicator background

Sea ice is frozen seawater that floats on the ocean surface. Sea-ice cover expands in Earth's polar regions each autumn and winter, as ocean water freezes in response to cooling of the atmosphere and ocean. Summer warming melts much of this seasonal ice, with annual sea-ice minima in each hemisphere typically occurring in late summer or early autumn (September in the northern hemisphere, February in the southern hemisphere). Changes in sea-ice cover affect ocean circulation, atmospheric dynamics and surface heating.

Sea-ice extent is the area of the ocean with at least 15% ice cover. This is a dynamic quantity, which changes in response to both thermodynamic growth (freezing) and decay (melting), as well as when the ice moves with winds and ocean currents. Sea-ice extent and sea-ice cover are mapped using microwave satellite imagery.

Long-term changes in Arctic sea-ice extent have been seen throughout the seasonal cycle. The downward trend in the minimum Arctic sea-ice extent from 1979 to 2024 is around 14% of the 1991–2020 average per decade, equivalent to a sea-ice loss of 77 000 km^2 per year.

Until 2015, Antarctic maximum sea-ice extent had a small but positive long-term trend. However, after recent low extents, that is no longer the case. While the last three years have had anomalously low Antarctic ice cover, it remains to be seen if there has been a regime shift in Antarctic sea-ice.[29]

Associated risks of declining sea-ice extent and the Sustainable Development Goals

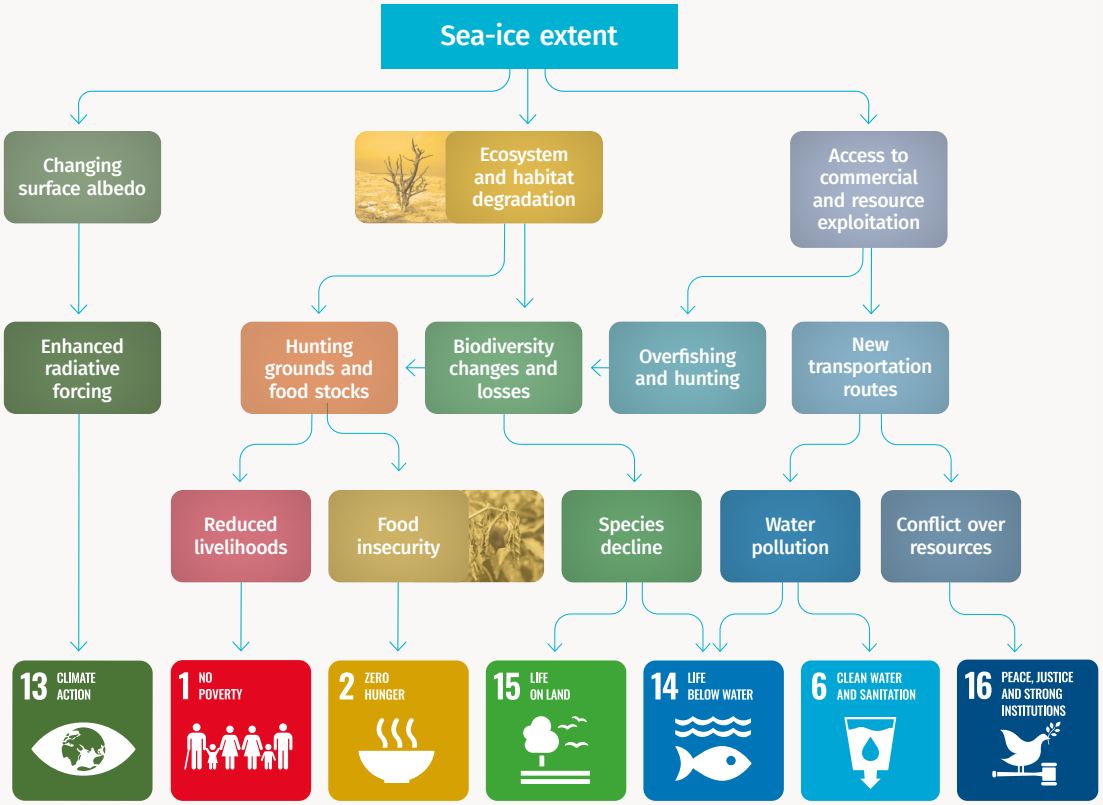

NEW KEY INDICATOR

Earth's energy imbalance

Key messages

The Earth's energy imbalance is a key climate indicator that measures how fast the heat trapped by anthropogenic emissions of greenhouse gases is accumulating in the climate system. The heat warms the ocean, continents and atmosphere, and melts ice.

The Earth's energy imbalance combines information about changes in all parts of the climate system in a comprehensive and holistic way, allowing a better quantification and prediction of changes in the climate system.

Since 1960, the Earth's energy imbalance has been increasing, particularly in the past 20 years compared to the previous 66 years.

Indicator background

The Earth's energy imbalance (EEI) is the difference between the amount of energy the Earth receives from the Sun (incoming solar radiation minus reflected solar radiation) and the amount of energy the Earth radiates back into space (outgoing long-wave radiation) (Figure 8). If the amount of incoming radiation exceeds the amount of outgoing radiation (for example, due to the greenhouse effect), the EEI is "positive", meaning the Earth is gaining energy, mostly in the form of heat. If more energy escapes the Earth than is received (for example, after large volcanic eruptions), the EEI is "negative", meaning the Earth is losing energy and cooling.

Due to increasing concentrations of greenhouse gases, the EEI has become increasingly positive over time, and the accumulation of surplus energy has led to warming of the climate.[30] Approximately 91% of the surplus energy has been absorbed by the ocean, 5% by the continents, 3% by the cryosphere and 1% by the atmosphere.

The EEI measures the rate of the heat accumulation and thus allows us to monitor the rate of global warming.[31,32,33] It provides a comprehensive picture of warming,[34,35] combining changes in all components of the climate system. It is therefore a crucial metric for assessing the state of the global climate system as well as testing our understanding and monitoring of it.[36]

The EEI can be measured in two ways:

1. The Earth heat inventory (1960–present). This method combines separate estimates of heat stored in the ocean, land and atmosphere, as well as the energy needed to melt ice. This hybrid approach integrates the Global Climate Observing System (satellite and in situ) data, reanalyses and climate models.[37]

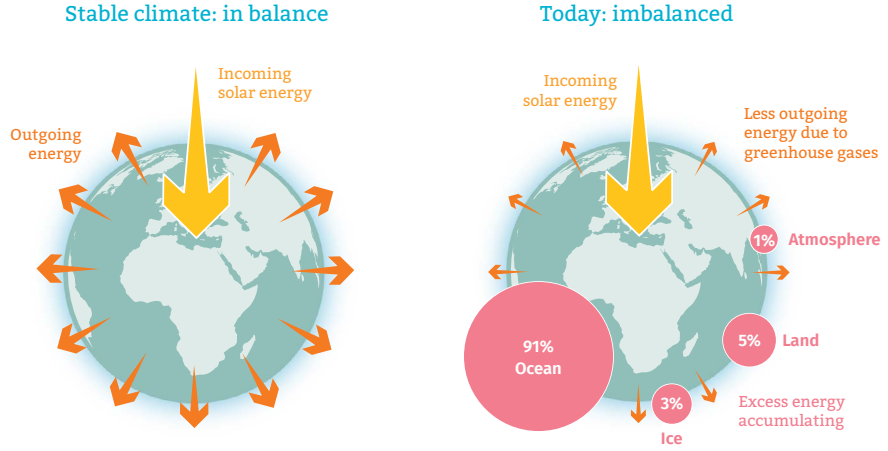

Figure 8. Schematic representation of the Earth's energy balance at the top of the atmosphere under a stable climate (left) where incoming solar radiation remains in quasi-equilibrium with the amount of outgoing energy, and under imbalanced conditions (right) where the amount of outgoing energy is reduced by increased concentrations of greenhouse gases, resulting today in an Earth climate that is out of energy balance. Consequently, heat is accumulating in the Earth's climate, of which about 91% is stored in the ocean, and the rest is going to warm the atmosphere and continents and to melt the ice.

Source: FAQ 7.1, IPCC, 2021[40]

A preliminary estimate of the inventory can be made using the observed ocean heat content.[38]

2. Direct satellite measurements (2000–present) of the incoming and outgoing radiation at the top of the atmosphere.[39]

State of the indicator

In 2025, the observed Earth energy imbalance (EEI) reached the highest value since the observational record began in 1960 (Figure 9a). Since 1960, heat has been accumulating in the Earth system, in the ocean, atmosphere, on land and in frozen regions of the planet, driven by a growing imbalance in the Earth's energy budget. As a result of the growing imbalance, the total amount of heat stored on Earth is not just increasing but accelerating. The rate of increase of EEI, as estimated from the ocean heat content, was 0.13 ± 0.03 W m^{-2} per decade for the period 1960–2025. It remained relatively stable over 1970–2025, 1980–2025 and 1990–2025 (Figure 9b), but was higher for the period 2001 to 2025 at 0.30 ± 0.1 W m^{-2} per decade.

For the period 2001–2025, EEI can also be measured directly by satellites. The rate of increase of EEI as measured by satellite over this period was 0.44 ± 0.13 W m^{-2} per decade (Figure 9b). The satellite estimate and the estimate based on ocean heat content are consistent within the joint margin of error for this period where they overlap.

These changes have been discussed in the literature.[41, 42, 43, 44, 45] The increase in EEI has been linked to rising concentrations of greenhouse gases and reductions in aerosol emissions.[46, 47, 48] It has also been linked to an increase in absorbed solar radiation associated with decreased reflection by clouds and sea ice, and a decrease in outgoing long-wave radiation due to increases in trace gases and water vapour.[49, 50]

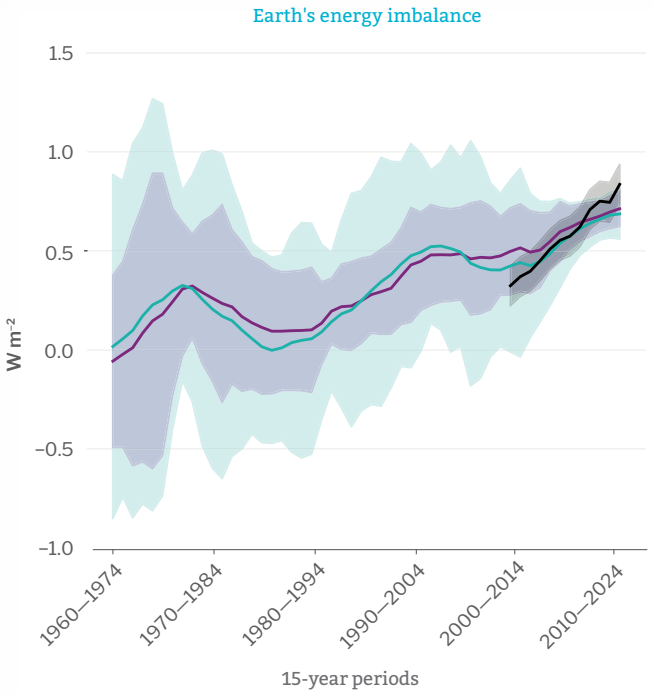

Figure 9a. Earth's energy imbalance time series estimated from ocean heat content (OHC) (purple and green), with values from remote-sensing at the top of the atmosphere (TOA, Loeb et al., 2021) anchored to the data from Minière et al. (2023). A positive EEI indicates that the total amount of heat stored on Earth is increasing.

OHC, von Schuckmann et al. (2023)
OHC, Minière et al. (2023)
TOA, Loeb et al. (2021)

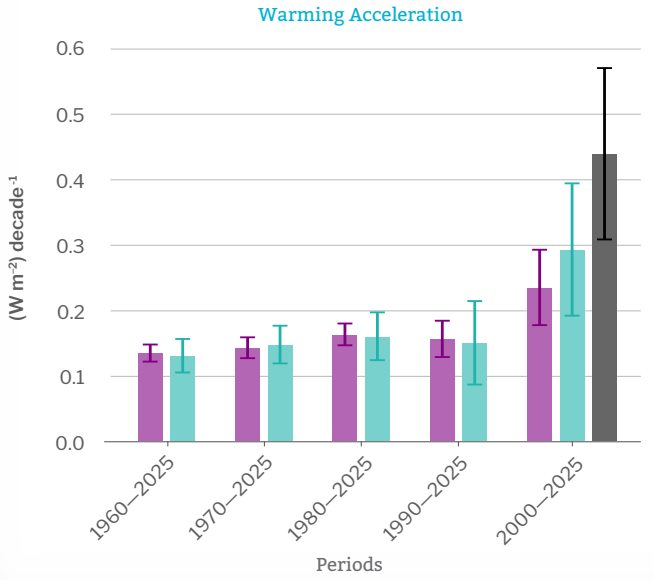

Figure 9b. Rate of change of the ocean-based estimates of EEI over various periods. Also shown is the rate of change of the EEI from remote-sensing at the top of the atmosphere (TOA) for the period 2001–2025. Ocean-based estimates are updated from von Schuckmann et al. (2023), and from Minière et al. (2023). A positive rate of change indicates that the total amount of heat stored on Earth is not just increasing but accelerating.

OHC, von Schuckmann et al. (2023)
OHC, Minière et al. (2023)
TOA, Loeb et al. (2021)

CLIMATE DRIVER

El Niño–Southern Oscillation

Key message

Weak La Niña conditions at the end of 2024 dissipated in early 2025 and neutral conditions prevailed until La Niña conditions re-emerged toward the end of 2025 and remained through to the end of the year.

State of El Niño–Southern Oscillation (ENSO)

Following the strong El Niño in 2023/2024, ENSO-neutral conditions began in April–June 2024 and generally prevailed until September–November 2025, with a brief dip into weak La Niña conditions[51] during late 2024 and early 2025. The weak La Niña conditions were relatively short lived with sea-surface temperature in the tropical Pacific returning to near normal levels early in the year. Sea-surface temperature anomalies in 2025 cooled once again in the latter half of the year, reaching the threshold of –0.5 °C for La Niña during the September–November period.

Monthly global temperatures in 2025 were generally lower than those of late 2023 and 2024, reflecting the shift from a strong El Niño event to neutral or weak La Niña conditions, but were generally higher than those of any pre-2023 year. The year 2025 thus became the warmest year without El Niño conditions on record.

Driver background

The El Niño–Southern Oscillation (ENSO) is one of the most important drivers of year-to-year and seasonal variability in weather patterns worldwide. It is linked to changes in the occurrence and distribution of hazards such as heavy rains, floods, drought, heatwaves (including marine heatwaves) and cold spells.

El Niño is characterized by higher-than-average sea-surface temperatures in the eastern tropical Pacific and a weakening of the trade winds in the region. The weakened trade winds reduce upwelling of cooler waters along the coast of South America, which in turn leads to higher sea-surface temperatures.

La Niña, which is characterized by below-average sea-surface temperatures in the central and eastern tropical Pacific and a strengthening of the trade winds, has effects that are generally the opposite of those of El Niño.

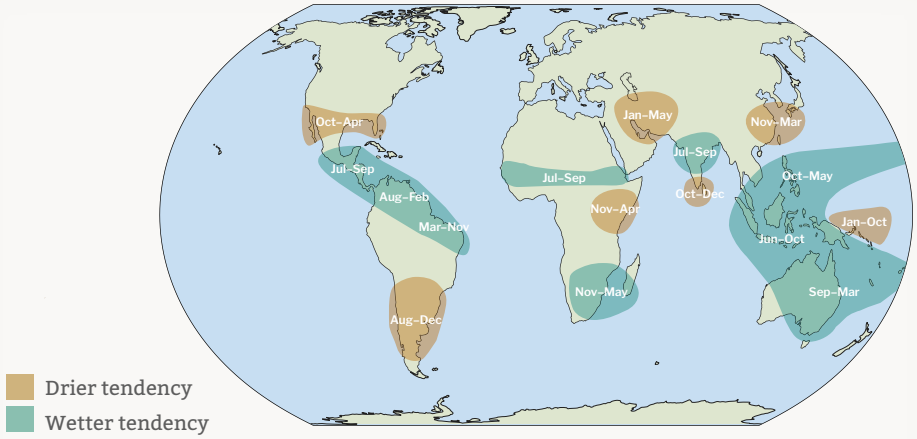

Figure 10. Typical La Niña seasonal precipitation effects during the year. Note that this is not a forecast; it is based on historical associations between La Niña and precipitation.

Source: Third-party map, may not fully align with United Nations and WMO map guidance. For details, see Datasets and Methods.

El Niño typically has a temporary warming influence on global average temperature, and La Niña generally has a temporary cooling influence. The greatest warming or cooling effects usually occur two to three months following the event peak because it takes time for the excess heating or cooling in the ocean to spread to and through the atmosphere.

El Niño and La Niña have an influence on regional rainfall patterns around the world, which can vary depending on the strength and timing of the event and other concurrent meteorological factors. Figure 10 shows some typical precipitation anomalies that are favoured by La Niña conditions. However, each La Niña is different, and other factors also influence rainfall.

The change in rainfall patterns can also affect global mean sea level, with higher global mean sea level during El Niño events and lower global mean sea levels during La Niña events.

Please refer to the sections on **Precipitation** and **High-impact weather and climate events** for more details of the events in 2025. Details on the evolution of ENSO can be found in the **WMO El Niño/La Niña Updates**.

CLIMATE DRIVER

Indian Ocean Dipole

Key message

The Indian Ocean Dipole was negative during most of 2025, reaching its third most negative index value in the 45-year record.

State of the Indian Ocean Dipole

The Indian Ocean Dipole was in its positive phase for much of 2023 and 2024, peaking toward the end of 2023 and reaching neutral conditions late in 2024 (Figure 11). In 2025, in contrast, the Indian Ocean Dipole was predominantly in its negative phase, from January until April and again from August to the end of the year, with neutral conditions in between. The index values during November were the third lowest since at least 1993, behind April 1999 and January 2011.

Driver background

The Indian Ocean Dipole (IOD), also known as the Dipole Mode Index (DMI), is a driver of rainfall and temperature variability in the Indian Ocean and neighbouring land masses, affecting rainfall over East Africa, the Arabian Peninsula, Indonesia and Australia, as well as influencing the strength of the Indian Monsoon. It also affects sea level along the coasts, changing the risk of coastal flooding.

The IOD index is calculated by taking the difference between sea-surface temperature anomalies in two areas, one in the east of the ocean basin (90°–110°E, 0°–10°S) and one in the west (50°–70°E, 10°S–10°N).

During the neutral phase, warm water flows from the Pacific into the Indian Ocean. Westerly winds blow along the Equator, with the air rising up over Indonesia and descending over the western part of the ocean basin.

The positive phase of the IOD is characterized by a weakening of the equatorial winds, allowing cooler, deeper water to reach the surface along the western coast of Sumatra and Java. This leads to higher-than-average sea-surface temperatures (SSTs) in the western Indian Ocean and lower-than-average sea-surface temperatures in the east. The change in SST affects the atmospheric circulation in the region, and during the positive phase the probability of rainfall is typically lower over Indonesia and parts of Australia, where sea-surface temperatures are lowered, and higher over East Africa, where they are raised. The south-west Arabian Peninsula in contrast, has a reduced chance of rainfall.[52]

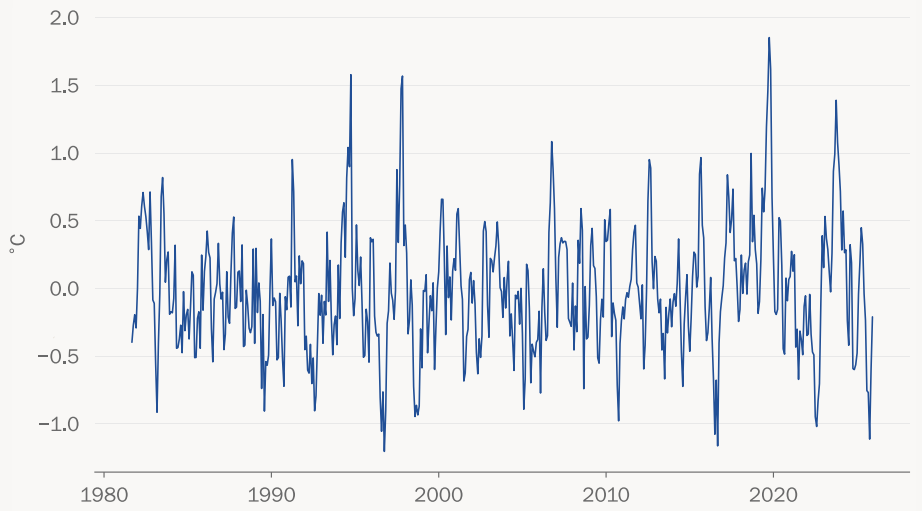

Figure 11. Monthly Indian Ocean Dipole index (difference from 1950–2000) average for the period 1981–2025.

Source: Data are from the National Oceanic and Atmospheric Administration Observing System Monitoring Center (NOAA OSMC)

In contrast, the negative phase of the IOD is characterized by a strengthening of the westerly winds, leading to lower-than-average sea-surface temperatures in the western Indian Ocean, together with a reduced probability of rainfall over East Africa, and higher-than-average sea-surface temperatures in the east, combined with increased chance of rainfall over Indonesia and Australia. The south-west Arabian Peninsula also sees an increased chance of rainfall.

The IOD and ENSO are linked. El Niño is often associated with, or can trigger, the positive phase of the IOD. La Niña is associated with the negative phase.

Global patterns of temperature and precipitation

Temperature

Averaged through 2025, near-surface temperatures were above the 1991–2020 average across most land areas, with only a few exceptions (Figure 12). Significant warm anomalies (see **Datasets and methods**) affected Greenland, northern Canada, western Europe, Fennoscandia and the Mediterranean as well as parts of western and central Asia and east Asia. Other areas of significant warmth included: parts of Central America and the Caribbean; western North America and Mexico; areas of tropical and northern Africa; southern Australia; southern South America; and an area centred on the Antarctic Peninsula. Only parts of India, southern Africa and a small area of South America were cooler than the long-term average.

Large areas of the ocean were also unusually warm, including: the northern and western Pacific, as well as more limited areas in the south; the southern and eastern Indian Ocean; and parts of the Atlantic Ocean, particularly the north-east.

Below average sea-surface temperatures were recorded in: the tropical Pacific, consistent with the La Niña conditions at the start and end of the year; the western Indian Ocean, consistent with the negative phase of the Indian Ocean Dipole (often associated with drier conditions over East Africa); limited areas of the Southern Ocean; and an area south of Greenland which is the only area of the world to have cooled on a century timescale.

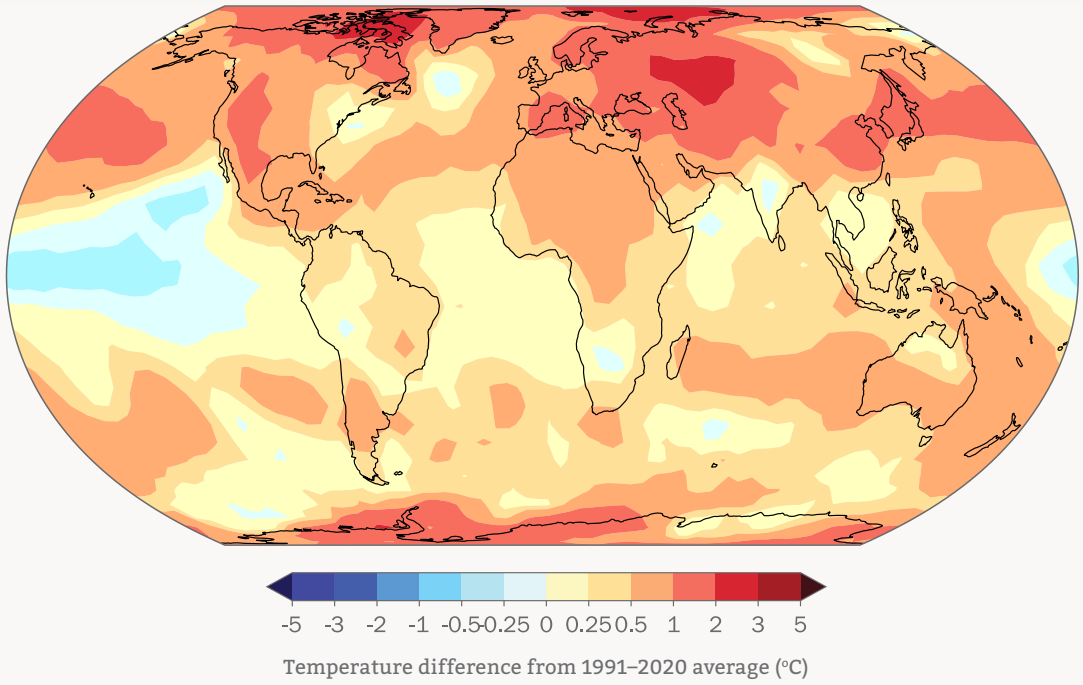

Figure 12. Annual average temperature anomalies for 2025 relative to the 1991–2020 average. The values shown are the median of nine global temperature datasets.

Source: Third-party map, may not fully align with United Nations and WMO map guidance.
For details, see "Annual Temperature Maps" in the Datasets and methods section.

Precipitation

In 2025, significantly drier-than-average conditions (below the 20th percentile of the 1991–2020 distribution of annual precipitation) were observed (Figure 13) over much of south-western Asia, around the Laptev Sea, in parts of eastern Africa and on the east African islands, as well as parts of Central Africa. North-western Africa has experienced a multi-year drought, although with some easing in late 2025. Unusually dry conditions were also observed northward of the Black Sea and in parts of central and western Europe. Drought conditions persisted in parts of the Amazon region and subtropical South America, although they eased in others. The Brazilian Highlands and parts of Patagonia were drier than usual. Other regions with unusually low precipitation amounts were located on the Greater Antilles, in northern North America, parts of southern Australia and on islands in the central Pacific.

Unusually wet conditions were observed in much of south and south-east Asia as well as northern Asia and parts of east Asia. It was the earliest monsoon onset over India since 2009.[53] Unusually high precipitation totals were also recorded in: parts of southern Africa and the Sahel region; the northern Andes; the central Gran Chaco, southern Pampa; eastern Mexico; areas of the Great Plains in North America; Alaska; and the Arctic regions of North America. Large areas of the Maritime Continent and islands south of the Equator in the western Pacific received unusually high precipitation amounts. In contrast, Pacific islands east of 150°E were unusually dry, a typical La Niña pattern.

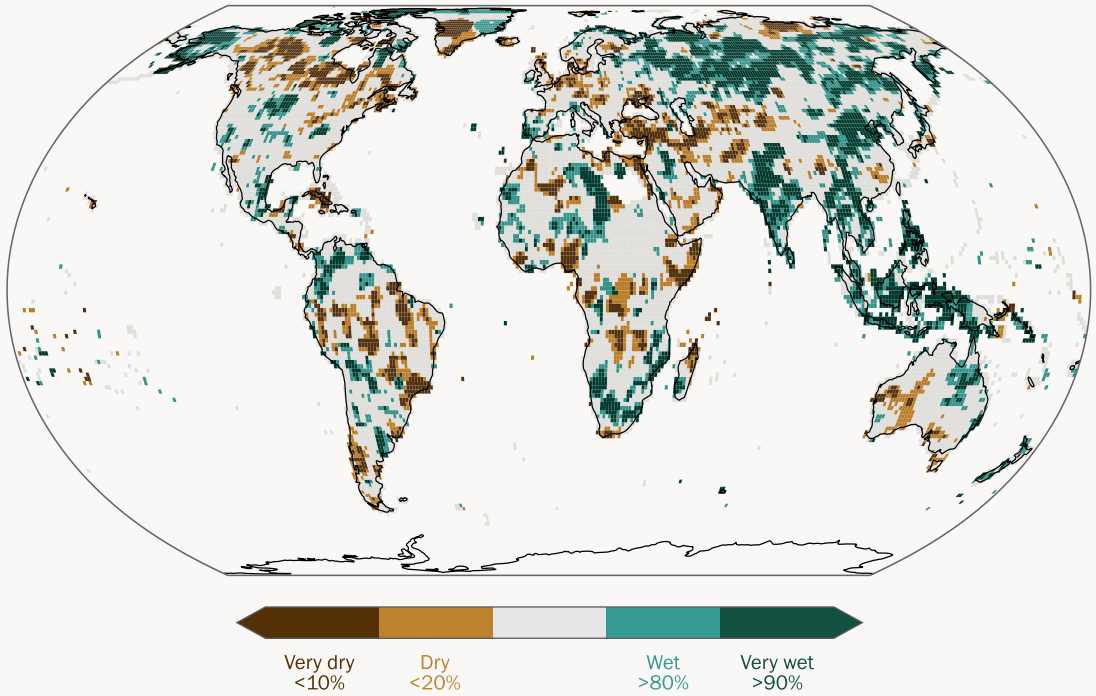

Figure 13. Annual precipitation 2025 expressed as percentiles of the 1991–2020 distribution. Brown areas are unusually dry. Green areas are unusually wet.

Source: Third-party map. Data for this map were provided by the Global Precipitation Climatology Centre (GPCC) and may not fully align with United Nations and WMO map guidance.

High-impact weather and climate events

Figure 14 highlights a selection of high-impact weather and climate events from 2025. It is based on input from WMO Members, the International Organization for Migration (IOM), Internal Displacement Monitoring Centre (IDMC), United Nations High Commissioner for Refugees (UNHCR), World Food Programme (WFP) and Food and Agriculture Organization of the United Nations (FAO), focusing on the meteorological aspects and the impacts related to displacement and food security. This represents only a small selection of the events of 2025; a wider range of events and their impacts can be found in the **Story Map** and **Extremes Supplement**.

High-impact weather and climate events arise when meteorological conditions combine with a particular vulnerability or vulnerabilities, leading to adverse impacts. Understanding the drivers of high-impact events involves understanding both the physical drivers and the underlying vulnerability, exposure and adaptive capacity of affected populations. Changes in the frequency or magnitude of such events can be related to changes in either one, or both.

The Summary for Policymakers of the Sixth Assessment Report (AR6) of the IPCC Working Group I concluded that:

> Widespread and rapid changes in the atmosphere, ocean, cryosphere and biosphere have occurred. Human-caused climate change is already affecting many weather and climate extremes in every region across the globe. This has led to widespread adverse impacts and related losses and damages to nature and people *(high confidence)*. Vulnerable communities who have historically contributed the least to current climate change are disproportionately affected *(high confidence)*.[54]

Extreme events have cascading impacts on agrifood systems. Recently, high temperatures, drought, flooding and price volatility have undermined agricultural production and access to healthy diets, especially in low- and middle-income countries.[55] Climate-driven food insecurity is now seen as a risk, with cascading effects on social stability, migration and biosecurity through the spread of plant pests and animal diseases.[56, 57]

Extreme weather, including flooding, droughts, cyclones, typhoons and hurricanes, continue to drive new, onward and protracted displacement of people globally, with particularly severe consequences in fragile and conflict-affected regions.[58] These events not only destroy homes, infrastructure and ecosystems, but also undermine resilience and pose serious protection risks to people on the move and those already living in displacement – many of whom are excluded from national preparedness and response plans.

Crucially, the cascading and compounding impacts of multiple, sequential disasters severely limit the ability of communities to prepare for, recover from and adapt to shocks. This is especially true in contexts where climate change intersects with conflict and insecurity, further deepening vulnerabilities and straining already overstretched local capacities.

Note that impact figures depend on the methods used to collect and process them. Therefore, they may not be directly comparable to statistics collected and processed in a different way.

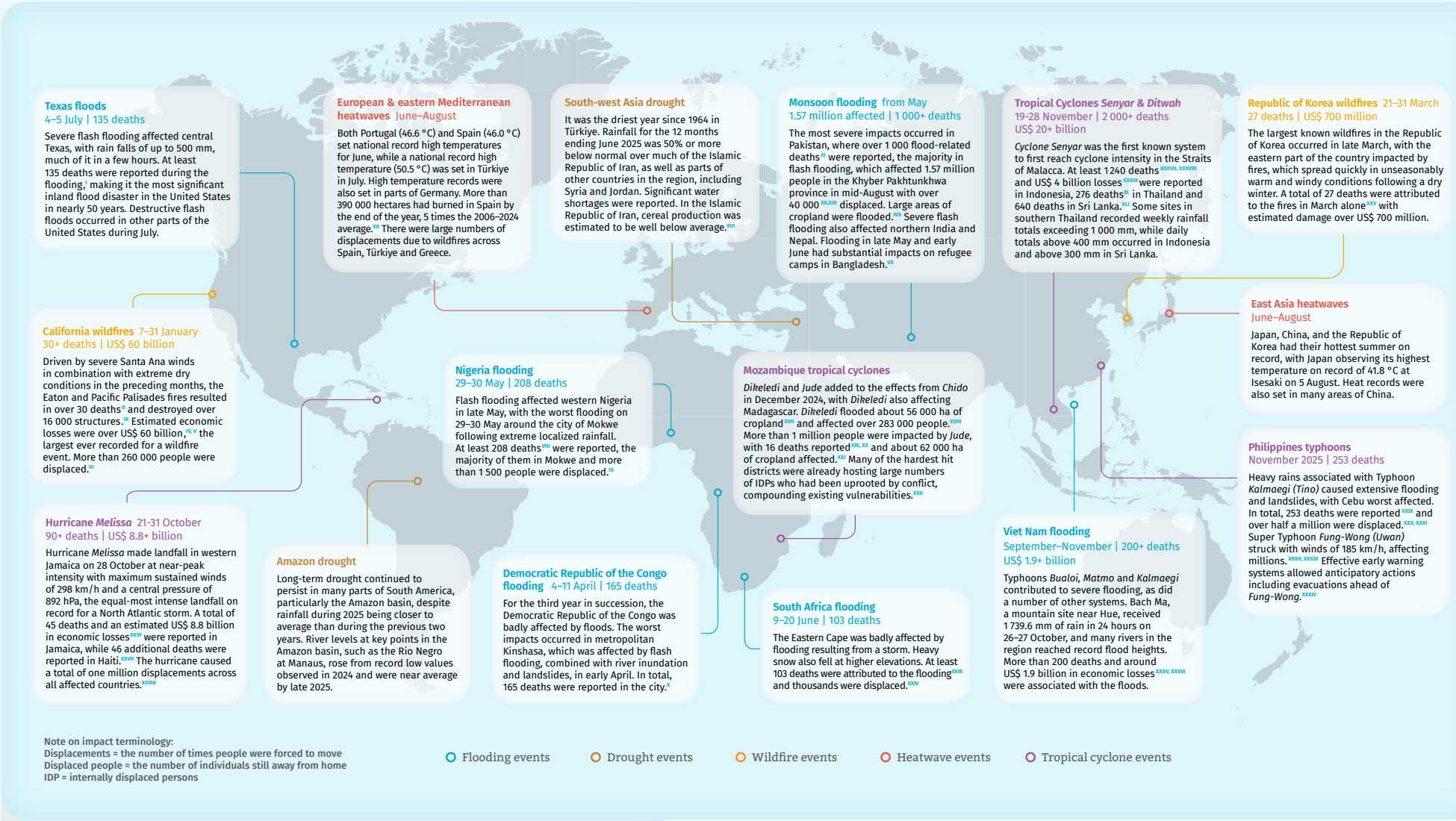

Figure 14. Extreme weather and climate events in 2025 had major global impacts.[59]

CASE STUDY

Climate and heat impacts on health

Human health is shaped by the changing climate. Rising temperatures, shifting rainfall patterns and changes in extremes are affecting where and when health risks emerge, how severe they become and who is most exposed. Extreme heat has wide-ranging impacts on mortality, livelihoods, ecosystems and health systems, while also amplifying risks such as vector- and water-borne diseases and mental health stressors.

Because many climate hazards are, to a degree, predictable, climate science and services provide a powerful foundation for anticipatory action, helping scientists to forecast health risks, prepare responses where diseases or impacts may occur and prevent avoidable harm.

While many climate-sensitive health risks deserve attention, this section highlights two of global concern – dengue and heat stress – and illustrates how climate data, early warning systems and integrated climate services for health can protect people and communities in a warming world.

Dengue: rising temperatures and expanding risk

Climate change is influencing both the geography and seasonality of infectious diseases that are sensitive to temperature and precipitation.[60] Vector-borne diseases are of particular concern, with dengue standing out as the world's fastest-growing mosquito-borne viral disease.[61]

According to the World Health Organization (WHO),[62] about half of the world's population is at risk of dengue, with an estimated 100–400 million infections occurring each year. Reported cases are currently the highest ever recorded.

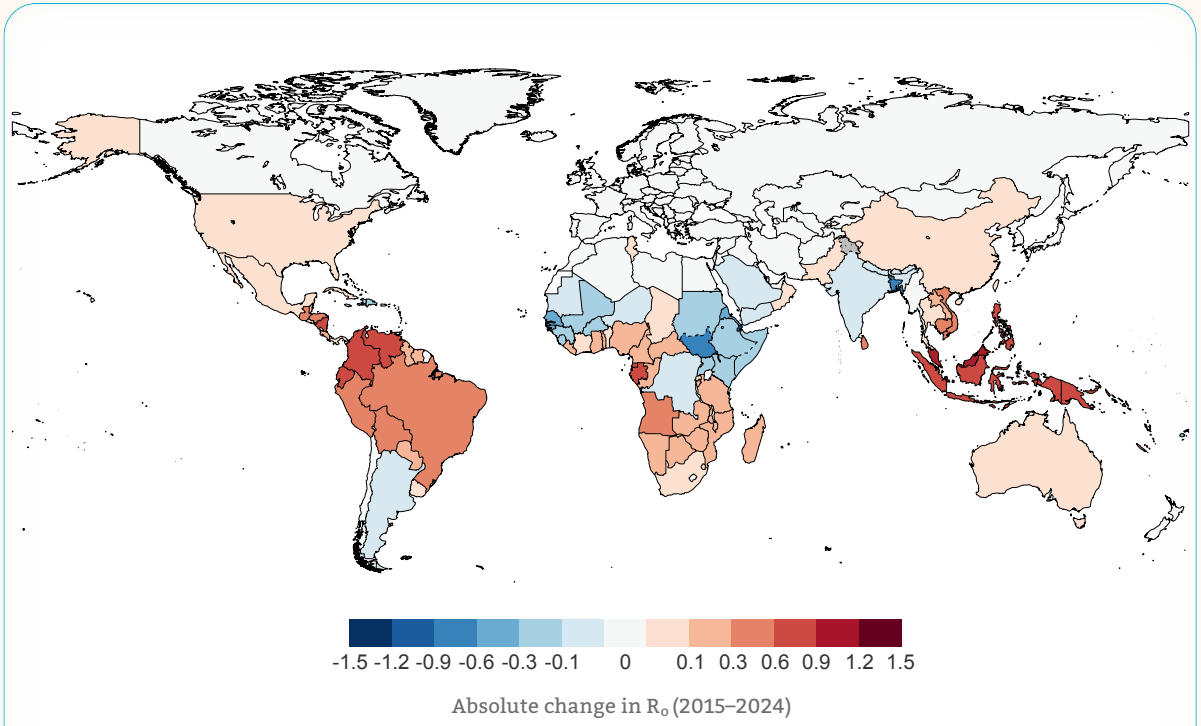

Figure 15. Climate suitability for the transmission of dengue. Absolute change in basic reproduction number (R_0) for dengue transmission by *Aedes aegypti* mosquitoes in 2015–2024, compared to a 1951–1960 baseline. R_0 is an indication of a pathogen's contagiousness and transmissibility.

Source: Third-party map. Data for this map originated from the 2025 Lancet Countdown report (available at lancetcountdown.org) and may not fully align with United Nations and WMO map guidance.

While dengue transmission is influenced by multiple social, environmental and health system factors, higher temperatures play a critical enabling role by amplifying vector efficiency, accelerating mosquito development, increasing biting rates and shortening viral incubation periods. Climate suitability for dengue transmission has increased substantially over recent decades (see Figure 15), with changes in rainfall patterns influencing breeding sites and population dynamics, expanding risk into new regions, and lengthening transmission seasons in areas where dengue is already endemic.

Chronic and extreme heat stress

While heat stress affects populations of all ages on all continents, workers are particularly vulnerable. Over one third of the global workforce (1.2 billion people) are exposed to workplace heat risk at some point each year, with those in agriculture and construction most affected. Rising temperatures increase fatigue, injuries, dehydration, kidney and mental strain, and productivity and livelihood losses.[63]

Recent guidance[64] from WHO and WMO calls on governments, employers, worker organizations and health authorities to take coordinated action, including: implementing heat-informed occupational policies; adapting work–rest schedules; ensuring access to shade, cooling and safe drinking water; strengthening worker training; and integrating weather and climate information into workplace risk management.

Heat-informed governance, planning and actions, and notably occupational health policies and protective measures, are needed to ensure maximum protection for workers worldwide.

Strengthening climate services for health: From early warnings to early action

Despite the scale of the risks, major gaps remain in preparedness and response. As of 2023, only around half of countries provide heat early warning services tailored to the needs of the health sector, and even fewer have fully integrated climate information into health decision-making processes.[65]

Climate-informed disease surveillance, early warning systems and predictive modelling are therefore essential tools for anticipating health risks and supporting timely public health action. Integrating meteorological and climate data with health information systems allows decision-makers to move from reactive outbreak response towards proactive prevention, targeted interventions, community engagement and health system preparedness.

WHO–WMO collaboration: Advancing integrated climate and health solutions

The WHO–WMO Joint Climate and Health Programme[66] plays a central role in advancing this integration by supporting partnerships and translating climate science into actionable and operational health intelligence.

Coordinated technical assistance and partnerships strengthen climate-informed health information systems, research, early warning systems and climate-resilient health services, aligned with global initiatives such as Early Warnings for All. These efforts help partners better use climate information to prevent, prepare for and respond to climate- and weather-related health risks, thereby protecting lives, reducing avoidable health burdens and safeguarding development gains.

Datasets and methods

Baselines

Baselines are periods of time, usually spanning three decades or more, that are used as a fixed benchmark against which current and future conditions can be compared. For scientific, policy and practical reasons, several different baselines are used in the present publication, and these are specified in the text and figures. Where possible, the most recent WMO climatological standard normal, 1991–2020, is used as the baseline for consistent reporting.

For some indicators, however, it is not possible to use the standard normal owing to a lack of measurements during the early part of the period. There are also two specific exceptions. First, for the global mean temperature time series – and only for the global mean series – a reference period of 1850–1900 is used. This is the baseline used by the Intergovernmental Panel on Climate Change (IPCC) Working Group I (WG I) in its contribution to the Sixth Assessment Report (AR6) as a reference period for pre-industrial conditions, and is relevant for understanding progress in the context of the Paris Agreement and other considerations in the United Nations Framework Convention on Climate Change. Second, greenhouse gas concentrations can be estimated much further back in time than 1850, using gas bubbles trapped in ice cores. The year 1750 is used in this report to represent pre-industrial greenhouse gas concentrations in line with IPCC AR6 WG I.

Atmospheric carbon dioxide

1 part per million (ppm) of CO_2 is equivalent to 7.8 Gt of CO_2 in the atmosphere.

Estimated concentrations from the year 1750 are used to represent pre-industrial conditions. Calculations assume a pre-industrial mole fraction of 278.3 ppm for CO_2, 729.2 part per billion (ppb) for CH_4 and 270.1 ppb for N_2O.[67]

Data and analysis from:

- World Data Centre for Greenhouse Gases operated by the Japan Meteorological Agency, **https://gaw.kishou.go.jp/**
- World Meteorological Organization (WMO). ***WMO Greenhouse Gas Bulletin – No. 21: The State of Greenhouse Gases in the Atmosphere Based on Global Observations through 2024***. Geneva, 2025.

Global mean near-surface temperature

— Global mean temperature series

The method for calculating global mean near-surface temperature anomalies relative to an 1850–1900 baseline is based on the assessment of long-term change and its uncertainty in IPCC AR6 WG I. In 2021, IPCC AR6 WG I assessed change from 1850–1900 to other periods based on an average of four datasets – HadCRUT5, Berkeley Earth, NOAA Interim and Kadow et al. (2020) – which start in 1850 and are globally or near-globally complete in the modern period.

To include shorter datasets, which can help to better understand recent temperature changes, in the present report, the estimate made by IPCC for the temperature change between 1850–1900 and 1981–2010 is combined with estimated changes between 1981–2010 and the current year from nine datasets – HadCRUT5, Berkeley Earth, NOAAGlobalTemp v6, GISTEMP v4, DCENT-I, CMST v3, CMA-GMST, ERA5 and JRA-3Q (for details of these see below) – to calculate anomalies for 2025 relative to 1850–1900. There is good agreement among the datasets on changes from 1981–2010 to the present, as this is a period with good observational coverage. The additional uncertainty from the spread of the datasets is combined with that of the IPCC's estimate of the uncertainty in the change from 1850–1900 to 1981–2010.

Global mean temperature anomalies were calculated relative to an 1850–1900 baseline using the following steps starting from the time series of global monthly mean temperatures for each dataset:

1. For each dataset, anomalies were calculated relative to the 1981–2010 average by subtracting the mean for the period 1981–2010 for each month separately.

2. An annual mean anomaly was calculated from the monthly mean anomalies.
3. The amount of 0.69 °C was added to each series, based on the estimated difference between 1850–1900 and 1981–2010, calculated using the method from IPCC AR6 WG I (see the caption for Figure 1.12 in that report).
4. The mean and standard deviation of the estimates were calculated.
5. The uncertainty in the IPCC estimate was combined with the standard deviation, assuming the two are independent and assuming the IPCC uncertainty range (0.54 °C–0.79 °C) is representative of a 90% confidence range (1.645 standard deviations).

The number quoted in this report for 2025 (1.43 °C ± 0.13 °C) was calculated in this way, with 1.43 °C being the mean of the nine estimates and 0.025 °C the standard deviation. The estimated uncertainty is quoted as a 90% uncertainty range.

— Annual temperature maps

For the map of temperature anomalies for 2025, a median of the available datasets was used, re-gridded to the spatial grid of the lowest resolution datasets (NOAAGlobalTemp, HadCRUT5, DCENT-I and CMST), which are presented on a 5° latitude by 5° longitude grid. The median is used in preference to the mean to minimize the effect of potential outliers in individual grid cells. The half-range of the datasets provides an indication of the uncertainty. The spread between the datasets is large at high latitudes and in Central Africa, both regions with sparse data coverage, and is generally larger over land than over the ocean.

Unusually high and low anomalies were identified based on the temperature rankings. Areas which were among the five warmest on record for the year were interpreted as unusually warm and areas which were among the five coldest on record were interpreted as unusually cold.

— Global mean temperature anomalies for 2025 relative to other periods

Table 1 shows global mean temperature anomalies for individual datasets for 2025 relative to four different baselines and their nominal ranking for 2025. The uncertainties indicated for the three modern baselines (1981–2010, 1991–2020 and 1961–1990) are the 90% uncertainty ranges. The following datasets were used, including seven traditional datasets:

Table 1. Global mean temperature dataset anomalies in °C and rankings for 2025 relative to different baselines

Period	1850–1900	1961–1990	1981–2010	1991–2020	Ranking
HadCRUT5	1.39	1.04	0.70	0.51	3
NOAAGlobalTemp	1.42	1.04	0.73	0.54	3
GISTEMP	1.45	1.09	0.76	0.57	2
Berkeley Earth	1.44	1.10	0.75	0.56	3
CMST	1.42	1.06	0.73	0.52	3
DCENT-I	1.44	1.09	0.75	0.56	2
CMA-GMST	1.41	1.04	0.72	0.52	3
ERA5	1.47	1.11	0.78	0.59	3
JRA-3Q	1.46	1.10	0.77	0.58	3
Mean of the nine datasets ± 90% uncertainty range	1.43 ± 0.13	1.08 ± 0.05	0.74 ± 0.04	0.55 ± 0.04	N/A

— Berkeley Earth: Rohde, R. A.; Hausfather, Z. The Berkeley Earth Land/Ocean Temperature Record. *Earth System Science Data* **2020**, *12* (4), 3469–3479. https://doi.org/10.5194/essd-12-3469-2020.

— GISTEMP v4: GISTEMP Team. *GISS Surface Temperature Analysis (GISTEMP), version 4*. NASA Goddard Institute for Space Studies, **2022**. https://data.giss.nasa.gov/gistemp/. Lenssen, N.; Schmidt, G.; Hansen, J. et al. Improvements in the GISTEMP Uncertainty Model. *Journal of Geophysical Research: Atmospheres* **2019**, *124* (12), 6307–6326. https://doi.org/10.1029/2018JD029522.

— HadCRUT.5.1.0.0: Morice, C. P.; Kennedy, J. J.; Rayner, N. A. et al. An Updated Assessment of Near-Surface Temperature Change From 1850: The HadCRUT5 Data Set. *Journal of Geophysical Research: Atmospheres* **2021**, *126* (3). https://doi.org/10.1029/2019JD032361. HadCRUT.5.1.0.0

data were obtained from http://www.metoffice.gov.uk/hadobs/hadcrut5 on 22 January 2026 and are © British Crown Copyright, Met Office 2026, provided under an Open Government Licence, https://www.nationalarchives.gov.uk/doc/open-government-licence/version/3/.

- NOAA v6: Huang, B.; Yin, X.; Menne, M. J. et al. *NOAA Global Surface Temperature Dataset (NOAAGlobalTemp), Version 6.0.0.* NOAA National Centers for Environmental Information, 2025. https://doi.org/10.25921/rzxg-p717.
- CMST v3: Sun, W.; Yang, Y.; Chao, L. et al. Description of the China Global Merged Surface Temperature version 2.0. *Earth System Science Data* **2022**, *14*, 1677–1693. https://doi.org/10.5194/essd-14-1677-2022.
- DCENT-I: Chan, D.; Chan, S. C.; Siddons, J. T. et al. *DCENT-I:* A *Globally Infilled Extension of the Dynamically Consistent Ensemble of Temperature Dataset.* Harvard Dataverse, 2025. https://doi.org/10.7910/DVN/ZY0WM8.

  Chan D.; Chan, S. C.; Siddons, J. T. et al. DCENT-I: A Globally Infilled Extension of the Dynamically Consistent ENsemble of Temperature Dataset. *Geoscience Data Journal* **2025**, *13* (2). https://doi.org/10.1002/gdj3.70054.
- CMA-GMST: Chen, L. ; Xu, W. ; Zhou, Z. et al. A New Global Land–Ocean Merged Surface Temperature Dataset Since the 1850s: The CMA-GMST Dataset. *Climate Dynamics* **2025**, *63*, 187. https://doi.org/10.1007/s00382-025-07614-x.

And two reanalyses:

- ERA5: Hersbach, H.; Bell, B.; Berrisford, P. et al. *ERA5 Monthly Averaged Data on Single Levels from 1940 to Present;* Copernicus Climate Change Service (C3S) Climate Data Store (CDS), 2023. https://doi.org/10.24381/cds.f17050d7.
- JRA-3Q: Kosaka, Y.; Kobayashi, S.; Harada, Y. et al. The JRA-3Q Reanalysis. *Journal of the Meteorological Society of Japan, Ser. II* **2024**, *102* (1), 49–109. https://doi.org/10.2151/jmsj.2024-004.

IPCC used an additional dataset:

- Kadow et al.: Kadow, C.; Hall, D. M.; Ulbrich, U. Artificial Intelligence Reconstructs Missing Climate Information. *Nature Geoscience* **2020**, *13*, 408–413. https://doi.org/10.1038/s41561-020-0582-5.

— Land surface air temperature

The land temperature assessment is based on six datasets:

- Berkeley Earth: Rohde, R.A.; Hausfather, Z. The Berkeley Earth Land/Ocean Temperature Record. *Earth System Science Data* **2020**, *12* (4), 3469–3479. https://doi.org/10.5194/essd-12-3469-2020.
- CMA-GLST: Chen, L.; Xu, W.; Zhou, Z. et al. A New Global Land–Ocean Merged Surface Temperature Dataset Since the 1850s: The CMA-GMST Dataset. *Climate Dynamics* **2025**, *63*, 187. https://doi.org/10.1007/s00382-025-07614-x.
- CLSAT 2.1: Wei, S.; Li, Q.; Xu, Q. et al. Updates to C-LSAT 2.1 and the Development of High-resolution Land Surface Air Temperature and Diurnal Temperature Range Datasets. *Earth System Science Data* **2025**, *17*, 4985–5005. https://doi.org/10.5194/essd-17-4985-2025.
- CRUTEM.5.1.0.0: Osborn, T.J.; Jones, P.D.; Lister, D.H. et al. Land Surface Air Temperature Variations Across the Globe Updated to 2019: The CRUTEM5 Data Set. *Journal of Geophysical Research* **2021**, 126 (2). https://doi.org/10.1029/2019JD032352. CRUTEM.5.1.0.0 data were obtained from https://www.metoffice.gov.uk/hadobs/crutem5 on 22 January 2026 and are © British Crown Copyright, Met Office 2026, provided under an Open Government Licence, http://www.nationalarchives.gov.uk/doc/open-government-licence/version/3/.
- DCENT-I: Chan, D.; Chan, S. C.; Siddons, J. T. et al. *DCENT-I: A Globally Infilled Extension of the Dynamically Consistent ENsemble of Temperature Dataset.* Harvard Dataverse, 2025. https://doi.org/10.7910/DVN/ZY0WM8.
- GHCNv4: Menne, M. J.; Williams, C. N.; Gleason, B. E. et al. The Global Historical Climatology Network Monthly Temperature Dataset, Version 4. *Journal of Climate* **2018**, *31*. https://doi.org/10.1175/JCLI-D-18-0094.1.

— Sea-surface temperature

The sea-surface temperature assessment is based on four datasets:

- CMA-SST: Chen, L.; Xu, W.; Zhou, Z. et al. A New Global Land–Ocean Merged Surface Temperature Dataset Since the 1850s: The CMA-GMST Dataset. *Climate Dynamics* **2025**, *63*, *187*. https://doi.org/10.1007/s00382-025-07614-x.

— HadSST.4.2.0.0: Kennedy, J.J.; Rayner, N. A.; Atkinson, C. P. et al. An Ensemble Data Set of Sea Surface Temperature Change from 1850: The Met Office Hadley Centre HadSST.4.0.0.0 Data Set. *Journal of Geophysical Research: Atmospheres* **2019**, *124* (14), 7719–7763. https://doi.org/10.1029/2018JD029867. HadSST.4.2.0.0 data were obtained from https://www.metoffice.gov.uk/hadobs/hadsst4 on 22 January 2026 and are © British Crown Copyright, Met Office 2026, provided under an Open Government Licence, http://www.nationalarchives.gov.uk/doc/open-government-licence/version/3/.

— DCENT-I: Chan, D.; Chan, S. C.; Siddons, J. T. et al. *DCENT-I: A Globally Infilled Extension of the Dynamically Consistent ENsemble of Temperature Dataset*. Harvard Dataverse, **2025**. https://doi.org/10.7910/DVN/ZY0WM8.

— ERSSTv6: Huang, B.; Yin, X.; Boyer, T. et al. Extended Reconstructed Sea Surface Temperature Version 6 (ERSSTv6). Part I: An Artificial Neural Network Approach. *Journal of Climate* **2025**, *38*, 1105–1121. https://doi.org/10.1175/JCLI-D-23-0707.1.

Huang, B.; Yin, X.; Boyer, T. et al. Extended Reconstructed Sea Surface Temperature Version 6 (ERSSTv6). Part II: Upgrades on Quality Control and Large-scale Filter. *Journal of Climate* **2025**, *38*, 1123–1136. https://doi.org/10.1175/JCLI-D-24-0185.1.

— Marine heatwaves and cold spells

Marine heatwaves are categorized as moderate when the sea-surface temperature (SST) is above the 90th percentile of the climatological distribution for five days or longer. The subsequent categories are defined in respect of the difference between the SST and the climatological distribution average: “strong”, “severe” or “extreme”, if that difference is, respectively, more than two, three or four times the difference between the 90th percentile and the climatological distribution average.

Marine cold spell categories are analogous but counting days below the 10th percentile.

The baseline used for marine heatwaves and cold spells is 1982–2011, which is shifted by one year from the *standard normal* period of 1981–2010 because the first full year of the satellite SST series on which it is based is 1982. This period has not been updated to the current standard normal period of 1991–2020 because the shifting of the baseline has a significant effect on the results and would not allow for comparison of marine heatwaves/marine cold spells statistics with previous versions of the present publication.

All marine heatwaves and cold spells are detected using the NOAA 0.25° Daily Optimum Interpolation Sea Surface Temperature (OISST) v2.1 dataset (Huang et al., 2021).

References

— Hobday, A. J.; Alexander, L. V.; Perkins, S. E. et al. A Hierarchical Approach to Defining Marine Heatwaves. *Progress in Oceanography* **2016**, *141*, 227–238. https://doi.org/10.1016/j.pocean.2015.12.014.

— Hobday, A. J.; Oliver, E. C J.; Sen Gupta, A. et al. Categorizing and Naming Marine Heatwaves. *Oceanography* **2018**, *31* (2), 1–13. https://www.jstor.org/stable/26542662.

— Huang, B.; Liu, C.; Banzon, V. et al. Improvements of the Daily Optimum Interpolation Sea Surface Temperature (DOISST) Version 2.1. *Journal of Climate* **2021**, *34* (8), 2923–2939. https://doi.org/10.1175/JCLI-D-20-0166.1.

— Schlegel, R. W.; Darmaraki, S.; Benthuysen, J. A. et al. Marine Cold-Spells. *Progress in Oceanography* **2021**, *198*. https://doi.org/10.1016/j.pocean.2021.102684.

Ocean heat content

Note that global ocean heat content (GOHC) values are given for the ocean surface area between 60°S and 60°N and limited to areas deeper than 300 m. A baseline of 2005–2025 is used for the ocean heat content time series as near-global coverage is available for this period thanks to the network of Argo subsurface floats. Warming rates in watts per square metre refer to the ocean surface area. To obtain a number for the entire surface of the globe (as used, for example, in the United Nations Educational, Scientific and Cultural Organization (UNESCO) *State of the Ocean* report) multiply by 0.71.

Ocean heat content changes are given in units of zettajoules (ZJ) per year. Changes can also be expressed in watts per square metre (1 W m–2 corresponds to 11.35 ZJ per year).

Table 2. Ocean warming rates from the main text in watts per square metre and zettajoules per year

Period	Depth range (m)	Rate in W m^{-2}	Rate in ZJ/year
2005–2025	0–2 000	1–1.17	11.0–12.2
1960–2005	0–2 000	0.29–0.37	3.05–3.91
1971–2025	0–2 000	0.66 ± 0.10	5.8 ± 0.5
1970–2025	2 000–6 000	0.1145 ± 0.0240	1.16 ± 0.24

Data sources

The IAP time series is available at http://www.ocean.iap.ac.cn/pages/dataService/dataService.html.

The Copernicus Marine OHC estimates are available and regularly updated at https://marine.copernicus.eu/ocean-climate-portal/ocean-heat-content.

The ensemble-based Minière et al. (2023) and von Schuckmann et al. (2023) time series have both been updated through 2025. Details of these updates and products used in both ensembles are described below.

Table 3. GOHC update details from von Schuckmann et al. (2023)

Product name	References	Time period
JMA	Ishii et al. (2017)	1960–2025
RFROM	Lyman and Johnson (2014)	1993–2025
NOC	Desbruyères et al. (2017)	2005–2025
IAP	Cheng et al. (2017)	1960–2025
Roemmich and Gilson (2009)	Roemmich and Gilson (2009)	2005–2025
EN.4.2.2.c14	Good et al. (2013)	1960–2025
CMEMS (CORA5.2)	Cabanes et al. (2013)	1960–2025
CMEMS (vS)	Von Schuckmann and Le Traon (2011)	2005–2025
LocalGP	Giglio et al. (2026)	2005–2025
MOAAv2 GPV	Hosoda et al. (2008); Hosoda (2007)	2005–2025
BOA-Argo	Li et al. (2017)	2005–2025
CSIRO-IIT-NOC (Hist)	Domingues et al. (2008) ; Church et al. (2011)	1970–2025, not limited to 60°S-60°N, > 300m bathymetry
CSIRO-GEOMAR-NOC (ARGO)		2005–2024
NCEI	Levitus et al. (2012)	1960–2025
Deep ocean	Johnson and Purkey (2024)	1988–2025 (using data from 1970-2025)

Table 4. GOHC update details from Minière et al. (2023)

Product name	References	Time period
JMA	Ishii et al. (2017)	1960–2024
RFROM	Lyman and Johnson (2023)	1960–2024
IAP	Cheng et al. (2017)	1960–2025
EN.4.2.2.C14	Good et al. (2013); Cheng et al. (2014)	1960–2025
EN.4.2.2.G10	Good et al. (2013); Gouretski and Reseghetti (2010)	1960–2025
EN.4.2.2.L09	Good et al. (2013); Levitus et al. (2009)	1960–2025
EN.4.2.2.C13	Good et al. (2013); Cowley et al. (2013)	1960–2025
CMEMS(CORA5.2)	Cabanes et al. (2013); Szekely et al. (2025)	1960–2025
CMEMS (vS)	Von Schuckmann and Le Traon (2011)	2005–2025
MOAAv2 GPV	Hosoda (2007); Hosoda et al. (2008)	2005–2025
BOA-Argo	Li et al. (2017)	2005–2025
ARMOR3D	Buongiorno Nardelli (2020)	1993–2025
SIO	Roemmich and Gilson (2009)	2005–2025
NOAA/NCEI	Levitus et al. (2012)	1960–2025
GDCSM	Zhang et al. (2022)	1960–2025

References

— Buongiorno Nardelli, B. A Multi-Year Time Series of Observation-Based 3D Horizontal and Vertical Quasi-Geostrophic Global Ocean Currents. *Earth System Science Data* **2020**, *12* (3), 1711–23. https://doi.org/10.5194/essd-12-1711-2020.

— Cabanes, C.; Grouazel, A.; Von Schuckmann, K. et al. The CORA Dataset: Validation and Diagnostics of In-Situ Ocean Temperature and Salinity Measurements. *Ocean Science* **2013**, *9* (1), 1–18. https://doi.org/10.5194/os-9-1-2013.

- Cheng, L.; Zhu, J.; Cowley, R. et al. Time, Probe Type, and Temperature Variable Bias Corrections to Historical Expendable Bathythermograph Observations. *Journal of Atmospheric and Oceanic Technology* **2014**, *31* (8), 1793–1825. https://doi.org/10.1175/JTECH-D-13-00197.1.
- Cheng, L.; Trenberth, K. E.; Fasullo, J. et al. Improved Estimates of Ocean Heat Content from 1960 to 2015. *Science Advances* **2017**, *3* (3). https://doi.org/10.1126/sciadv.1601545.
- Church, J. A.; White, N. J.; Konikow, L.F. et al. Revisiting the Earth's Sea-Level and Energy Budgets from 1961 to 2008. *Geophysical Research Letters* **2011**, *38* (18). https://doi.org/10.1029/2011GL048794.
- Cowley, R.; Wijffels, S.; Cheng, L. Biases in Expendable Bathythermograph Data: A New View Based on Historical Side-by-Side Comparisons. *Journal of Atmospheric and Oceanic Technology* **2013**, *30* (6), 1195–225. https://doi.org/10.1175/JTECH-D-12-00127.1.
- Desbruyères, D.; McDonagh, E. L.; King, B. A. et al. Global and Full-Depth Ocean Temperature Trends during the Early Twenty-First Century from Argo and Repeat Hydrography. *Journal of Climate* **2017**, *30* (6), 1985–1997. https://doi.org/10.1175/JCLI-D-16-0396.1.
- Domingues, C. M.; Church, J. A.; White, N. J. et al. Improved Estimates of Upper-Ocean Warming and Multi-Decadal Sea-Level Rise. *Nature* **2008**, *453* (7198), 1090–1093. https://doi.org/10.1038/nature07080.
- Giglio, D.; Sukianto, T.; Kuusela, M. et al. Global Ocean Heat Content Anomalies and Ocean Heat Uptake Based on Mapping Argo Data Using Local Gaussian Processes. *Zenodo*, 1 February 2026, Version 4.0.1. https://doi.org/10.5281/ZENODO.18187866.
- Good, S. A.; Martin, M. J.; Rayner, N. A. EN4: Quality Controlled Ocean Temperature and Salinity Profiles and Monthly Objective Analyses with Uncertainty Estimates. *Journal of Geophysical Research: Oceans* **2013**, *118* (12), 6704–6716. https://doi.org/10.1002/2013JC009067.
- Gouretski, V.; Reseghetti. F. On Depth and Temperature Biases in Bathythermograph Data: Development of a New Correction Scheme Based on Analysis of a Global Ocean Database. *Deep Sea Research Part I: Oceanographic Research Papers* **2010**, *57* (6), 812–833. https://doi.org/10.1016/j.dsr.2010.03.011.
- Hosoda, S. *Grid Point Value of the Monthly Objective Analysis Using the Argo Data*. JAMSTEC, 2007. https://doi.org/10.17596/0000102.
- Hosoda, S.; Ohira, T.; Nakamura, T. A Monthly Mean Dataset of Global Oceanic Temperature and Salinity Derived from Argo Float Observations. *JAMSTEC Report of Research and Development* **2008**, *8*, 47–59. https://doi.org/10.5918/jamstecr.8.47.
- Ishii, M.; Fukuda, Y.; Hirahara, S. et al. Accuracy of Global Upper Ocean Heat Content Estimation Expected from Present Observational Data Sets. *SOLA* **2017**, *13*, 163–167. https://doi.org/10.2151/sola.2017-030.
- Johnson, G. C.; Purkey, S. G. Refined Estimates of Global Ocean Deep and Abyssal Decadal Warming Trends. *Geophysical Research Letters* 2**024**, *51* (18). https://doi.org/10.1029/2024GL111229.
- Levitus, S.; Antonov, J. I.; Boyer, T. P. et al. Global Ocean Heat Content 1955–2008 in Light of Recently Revealed Instrumentation Problems. *Geophysical Research Letters* **2009**, *36* (7). https://doi.org/10.1029/2008GL037155.
- Levitus, S.; Antonov, J. I.; Boyer, T. P. et al. World Ocean Heat Content and Thermosteric Sea Level Change (0–2 000 m), 1955–2010. *Geophysical Research Letters* **2012**, *39* (10). https://doi.org/10.1029/2012GL051106.
- Li, H.; Xu, F.; Zhou, W. et al. Development of a Global Gridded Argo Data Set with Barnes Successive Corrections. *Journal of Geophysical Research: Oceans* **2017**, *122* (2), 866–89. https://doi.org/10.1002/2016JC012285.
- Lyman, J. M.; Johnson, G. C. Global High-Resolution Random Forest Regression Maps of Ocean Heat Content Anomalies Using In Situ and Satellite Data. *Journal of Atmospheric and Oceanic Technology* **2023**, *40 (5)*, 575-586. https://doi.org/10.1175/JTECH-D-22-0058.1.
- Lyman, J. M.; Johnson, G. C. Estimating Global Ocean Heat Content Changes in the Upper 1800 m since 1950 and the Influence of Climatology Choice. *Journal of Climate* **2014**, *27* (5), 1945–1957. https://doi.org/10.1175/JCLI-D-12-00752.1.
- Minière, A.; von Schuckmann, K.; Sallée, J.-B. et al. Robust Acceleration of Earth System Heating Observed over the Past Six Decades. *Scientific Reports* **2023**, *13* (1). https://doi.org/10.1038/s41598-023-49353-1.
- Roemmich, D.; Gilson, J. The 2004–2008 Mean and Annual Cycle of Temperature, Salinity, and Steric Height in the Global Ocean from the Argo Program. *Progress in Oceanography* **2009**, *82* (2), 81–100. https://doi.org/10.1016/j.pocean.2009.03.004.

— Szekely, T.; Gourrion, J.; Pouliquen, S. et al. *CORA, Coriolis Ocean Dataset for Reanalysis*. SEANOE, 2025. https://doi.org/10.17882/46219.

— Von Schuckmann, K.; Le Traon, P.-Y. How Well Can We Derive Global Ocean Indicators from Argo Data? *Ocean Science* **2011**, *7* (6), 783–91. https://doi.org/10.5194/os-7-783-2011.

— Von Schuckmann, K.; Minière, A.; Gues, F. et al. Heat Stored in the Earth System 1960–2020: Where Does the Energy Go? *Earth System Science Data* **2023**, *15* (4), 1675–1709. https://doi.org/10.5194/essd-15-1675-2023.

— Zhang, C.; Wang, D. Liu, Z. et al. Global Gridded Argo Dataset Based on Gradient-Dependent Optimal Interpolation. *Journal of Marine Science and Engineering* **2022**, 10 (5), 650. https://doi.org/10.3390/jmse10050650.

Global mean sea level

Global mean sea level data are from Centre national d'études spatiales (CNES)/Aviso+, https://www.aviso.altimetry.fr/en/data/products/ocean-indicators-products/mean-sea-level/data-acces.html#c12195.

Ocean pH

This indicator is produced by the Copernicus Marine Service. References include:

— Chau, T. T. T.; Gehlen, M.; Chevallier, F. A. Seamless Ensemble-based Reconstruction of Surface Ocean pCO2 and Air–Sea CO_2 Fluxes over the Global Coastal and Open Oceans. *Biogeosciences* **2022**, *19*, 1087–1109. https://doi.org/10.5194/bg-19-1087-2022.

— Gehlen M.; Chau, T. T. T.; Conchon, A. et al. Ocean Acidification. In Copernicus Marine Service Ocean State Report, Issue 4; Von Schuckmann, K.; Le Traon, P.-Y.; Smith, N. et al., Eds. *Journal of Operational Oceanography* **2020**, *13* [special supplement), s88–s91. https://doi.org/10.1080/1755876X.2020.1785097.

Glacier mass balance

Global glacier monitoring information is provided by the World Glacier Monitoring Service:

— World Glacier Monitoring Service (WGMS). *Fluctuations of Glaciers (FoG) Database*. WGMS: Zurich, Switzerland, 2026. https://doi.org/10.5904/wgms-fog-2024-01.

Sea-ice extent

Data are from:

— The European Organization for the Exploitation of Meteorological Satellites (EUMETSAT) Ocean and Sea Ice Satellite Application Facility (OSI SAF) Sea-Ice Index v2.3 (based on Lavergne et al., 2019);

— The National Snow and Ice Data Center (NSIDC) v4 Sea Ice Index (Fetterer et al., 2017);

— JAXA (Krishfield et al., 2014).

Sea-ice concentrations are estimated from microwave radiances measured from satellites. Extent is the area of ocean grid cells where the sea-ice concentration exceeds 15%. There are modest differences in the absolute extent between datasets, but they agree well on the year-to-year changes and trends.

In the main text of the present report, an average of the three observed datasets is reported for extents, and rankings are given as the range of rankings from the three datasets. Uncertainty is estimated as the largest absolute difference between the mean and each individual dataset. Values for NSIDC, OSI SAF and JAXA are given separately in Tables 5 and 6.

References

— European Organization for the Exploitation of Meteorological Satellites (EUMETSAT) Ocean and Sea Ice Satellite Application Facility (OSI SAF). *Sea Ice Index 1978–Onwards, Version 2.3, OSI 420*. EUMETSAT OSI SAF, 2025. Data extracted from OSI SAF FTP server: (1978–2025). https://osisaf-hl.met.no/v2p3-sea-ice-index.

— Fetterer, F.; Knowles, K.; Meier, W. N. et al. *Sea Ice Index, Version 3*. National Snow and Ice Data Center (NSIDC): Boulder, USA, 2017. https://nsidc.org/data/G02135/versions/3.

— Krishfield, R. A.; Proshutinsky, A.; Tateyama, K. et al. Deterioration of Perennial Sea Ice in the Beaufort Gyre from 2003 to 2012 and Its Impact on the Oceanic Freshwater Cycle. *Journal of Geophysical Research Oceans* **2014**, *119*. https://doi.org/10.1002/2013JC008999.

— Lavergne, T.; Sørensen, A. M.; Kern, S. et al. Version 2 of the EUMETSAT OSI SAF and ESA CCI Sea-ice Concentration Climate Data Records. *The Cryosphere* **2019**, *13* (1), 49–78. https://doi.org/10.5194/tc-13-49-2019.

Table 5. Arctic sea-ice extent statistics compared between NSIDC, EUMETSAT OSI SAF and JAXA for 2025

Metric	NSIDC v4 in million km²	OSI SAF v2p3 in million km²	JAXA in million km²
Annual minimum 2025 (anomaly with respect to 1991–2020) and date	4.54 (–0.83) 8.9.2025	5.09 (–0.61) 7.9.2025	4.58 (–0.76) 7.9.2025
Annual maximum 2025 (anomaly with respect to 1991–2020) and date	14.35 (–0.91) 21.3.2025	14.42 (–0.83) 20.3.2025	13.79 (–0.90) 20.3.2025
Annual average 2025 (anomaly with respect to 1991–2020)	10.12 (–0.96)	10.39 (–0.84)	9.75 (–0.97)
Annual minimum 1991–2020 average	5.37	5.70	5.34
Annual maximum 1991–2020 average	15.26	15.25	14.69
Annual average 1991–2020 average	11.08	11.23	10.72

Table 6. Antarctic sea-ice extent statistics compared between NSIDC, EUMETSAT OSI SAF and JAXA for 2025

Metric	NSIDC v4 in million km²	OSI SAF v2p3 in million km²	JAXA in million km²
Annual minimum 2025 (anomaly with respect to 1991–2020) and date	1.96 (–0.88) 1.3.2025	2.12 (–0.96) 25.2.2025	2.11 (–0.77) 23.2.2025
Annual maximum 2025 (anomaly with respect to 1991–2020) and date	17.85 (–1.05) 15.9.2025	18.28 (–0.98) 15.9.2025	17.88 (–0.96) 15.9.2025
Annual average 2025 (anomaly with respect to 1991–2020)	10.78 (–0.91)	11.20 (–0.87)	10.87 (–0.81)
Annual minimum 1991–2020 average	2.84	3.08	2.88
Annual maximum 1991–2020 average	18.90	19.26	18.84
Annual average 1991–2020 average	11.70	12.07	11.68

Climate driver: El Niño–Southern Oscillation

The map of typical La Niña seasonal precipitation effects is a composite from a number of sources:

- https://science.nasa.gov/earth/earth-observatory/la-nina-returns-for-a-second-winter-149201/
- https://iridl.ldeo.columbia.edu/maproom/IFRC/FIC/laninarain.html
- https://www.metoffice.gov.uk/research/climate/seasonal-to-decadal/gpc-outlooks/el-nino-la-nina
- https://ds.data.jma.go.jp/tcc/tcc/products/climate/ENSO/lanina.html
- https://journals.ametsoc.org/view/journals/hydr/24/1/JHM-D-22-0043.1.xml
- https://confluence.ecmwf.int/display/COPSRV/ENSO+impacts+on+Europe

Climate driver: Indian Ocean Dipole

The data for the Indian Ocean Dipole time series are from: https://stateoftheocean.osmc.noaa.gov/sur/ind/dmi.php

Calculated using sea-surface temperature data from:

— Huang, B.; Liu, C.; Banzon, V. et al. Improvements of the Daily Optimum Interpolation Sea Surface Temperature (DOISST) Version 2.1. *Journal of Climate* **2021**, *34*, 2923–2939. https://doi.org/10.1175/JCLI-D-20-0166.1.

Annual precipitation map

The map for the precipitation quantiles of 2025 is based on data from the Global Precipitation Climatology Centre (GPCC). Data for 2025 and reference data, to rank the 2025 annual total, were taken from the GPCC Monthly Product (https://opendata.dwd.de/climate_environment/GPCC/html/gpcc_precipitation_analysis_monthly_v2025_doi_download.html) for the years 1991 to 2020. A spatial resolution of 1° latitude/longitude was used.

Earth's energy imbalance

The Earth heat inventory is available at https://doi.org/10.26050/WDCC/GCOS_EHI_EXP_v2 (von Schuckmann et al., 2023). For details on the ocean heat content (OHC) time series used to derive the Earth's energy imbalance (EEI) from Minière et al. (2023) and von Schuckmann et al. (2023), please refer to Ocean heat content.

The EEI from remote-sensing at the top of the atmosphere (TOA) is obtained from the CERES EBAF TOA product (net radiative flux, available at https://ceres.larc.nasa.gov/data/; Loeb et al., 2021).

EEI time series from OHC and the corresponding acceleration estimates (panel (b) of Figure 9) were computed following the methodology described in Minière et al. (2023).

References

— Loeb, N. G.; Johnson, G. C.; Thorsen, T. J. et al. Satellite and Ocean Data Reveal Marked Increase in Earth's Heating Rate. *Geophysical Research Letters* **2021**, *48* (13). https://doi.org/10.1029/2021GL093047.

— Minière, A.; von Schuckmann, K.; Sallée, J.-B. et al. Robust Acceleration of Earth System Heating Observed over the Past Six Decades. *Scientific Reports* **2023**, *13* (1). https://doi.org/10.1038/s41598-023-49353-1.

— von Schuckmann, K.; Minière, A.; Gues, F. et al. Heat Stored in the Earth System 1960–2020: Where Does the Energy Go? *Earth System Science Data* **2023**, *15* (4), 1675–1709. https://doi.org/10.5194/essd-15-1675-2023.

Contributors

Contributing Members

Antigua and Barbuda; Argentina; Australia; Azerbaijan; Bahrain; Bangladesh; Belarus; Belgium; Belize; Bosnia and Herzegovina; Botswana; Brazil; Brunei Darussalam; Bulgaria; Canada; Chad; Chile; China; Croatia; Cuba; Cyprus; Czechia; Denmark; Dominica; Dominican Republic; El Salvador; Estonia; Eswatini; Finland; France; Georgia; Honduras; Hong Kong, China; Hungary; Iceland; India; Ireland; Israel; Italy; Jamaica; Japan; Jordan; Kazakhstan; Latvia; Libya; Lithuania; Luxembourg; Macao, China; Malawi; Malaysia; Mali; Mexico; Morocco; Moldova (Republic of); Myanmar; Namibia; Netherlands (Kingdom of the); New Caledonia; New Zealand; North Macedonia; Norway; Pakistan; Panama; Paraguay; Peru; Portugal; Republic of Korea; Saudi Arabia; Senegal; Serbia; Seychelles; Singapore; Slovakia; Slovenia; South Africa; Spain; Sweden; Switzerland; Syrian Arab Republic; Thailand; Tunisia; Türkiye; United Kingdom of Great Britain and Northern Ireland; United Republic of Tanzania; United States of America; Uruguay; Venezuela (Bolivarian Republic of); Viet Nam

Institutions

Agencia Estatal de Meteorología (AEMET), Spain; Bureau of Meteorology (BOM), Australia; CELAD, France; École normale supérieure (ENS), France; Egyptian Meteorological Authority; Environment and Climate Change Canada (ECCC); European Centre for Medium-Range Weather Forecasts (ECMWF); Global Precipitation Climatology Centre (GPCC), Germany; Graduate School of International Studies (GSIS), Korea University; Instituto Nacional de Meteorologia (INMET), Brazil; Internal Displacement Monitoring Centre (IDMC); Japan Meteorological Agency (JMA); Kenya Meteorological Department (KMD); Koninklijk Nederlands Meteorologisch Instituut (KNMI), Netherlands (Kingdom of the); Korea Meteorological Administration, Republic of Korea; Laboratoire d'Etudes en Géophysique et Océanographie Spatiales (LEGOS), France; Laboratoire de Météorologie Dynamique (LMD), France; Mercator Ocean international, France; Met Office Hadley Centre, UK; Météo-France; National Center for Meteorology (NCM), Saudi Arabia; NOAA National Centers for Environmental Information (NCEI), USA; Royal Meteorological Institute of Belgium (RMI); Saint Vincent and the Grenadines Meteorological Service; Turkish State Meteorological Service (TSMS); Universidade Estadual Paulista/Centro Nacional de Monitoramento e Alertas de Desastres Naturais (UNESP/CEMADEN), Brazil; Universidade Federal do Rio de Janeiro (UFRJ), Brazil; University of Bristol, UK; World Data Centre for Greenhouse Gases (WDCGG); World Glacier Monitoring Service (WGMS)

United Nations agencies

Food and Agriculture Organization of the United Nations (FAO), International Organization for Migration (IOM), United Nations High Commissioner for Refugees (UNHCR), World Food Programme (WFP)

Section authors

Lead author and scientific coordinator – John Kennedy (WMO)

Key indicator: atmospheric carbon dioxide – Oksana Tarasova (WMO)

Key indicator: global mean near-surface temperature – John Kennedy (WMO)

Key indicator: ocean heat content – Karina von Schuckmann (Mercator Ocean International), Audrey Minière (ENS, LMD), Flora Gues (CELAD), Christopher P. Atkinson (Met Office Hadley Centre), Lijing Cheng (Institute of Atmospheric Physics), John A. Church (Climate Change Research Centre, University of New South Wales), Damien Desbruyères (University of Brest, Centre national de la recherche scientifique (CNRS), Institut français de recherche pour l'exploitation de la mer (IFREMER), Institut de recherche pour le développement (IRD), Laboratoire d'Océanographie Physique et Spatiale (LOPS), Institut Universitaire Européen de la Mer (IUEM)), Catia M. Domingues (National Oceanography Centre), Donata Giglio (University of Colorado Boulder), Gregory C. Johnson (School of Oceanography, University of Washington and NOAA/Pacific Marine Environmental Laboratory), Rachel E. Killick (Met Office Hadley Centre), Brian King (National Oceanography Centre), Mikael Kuusela (Carnegie Mellon University), John M. Lyman (University of Hawaii), Bill Katie-Anne Mills (University of Colorado), Masatoshi Miyamoto (Japan Meteorological Agency), Didier P. Monselesan (Commonwealth Scientific and Industrial Research Organisation (CSIRO)), Sarah G. Purkey (Scripps Institution of Oceanography), James Reagan (NOAA NCEI), Abhishek Savita (Indian Institute of Technology Delhi), Thea Sukianto (Carnegie Mellon University), Tanguy Szekely (OceanScope), Susan E. Wijffels (Woods Hole Oceanographic Institution)

Key indicator: global mean sea level – Anny Cazenave (LEGOS), Lancelot Leclerq (LEGOS)

Key indicator: ocean pH – Karina von Schuckmann (Mercator Ocean international), Flora Gues (CELAD)

Key indicator: glacier mass balance – Shawn Marshall (ECCC)

Key indicator: sea-ice extent – Shawn Marshall (ECCC)

Climate driver: El Niño–Southern Oscillation – Jessica Blunden (NOAA NCEI)

Climate driver: Indian Ocean Dipole – John Kennedy (WMO), Jessica Blunden (NOAA NCEI)

Global patterns of temperature and precipitation – Markus Ziese (GPCC, Deutsche Wetterdienst), John Kennedy (WMO)

High-impact weather and climate events – Blair Trewin (BOM), Jana Birner (UNHCR), Hideki Kanamaru (FAO), Yang Feiyun (China Meteorological Administration (CMA) Training Centre), Andrea Setti (FAO), Caroline Kirungu (FAO), Theodore Allen (FAO), Freja Vamborg (ECMWF), Helena De Jong (IOM), Esmé O'Keeffe (UNHCR), Giancarlo Pini (WFP), Ivana Hajzmanova (IDMC), Yichen Shen (IOM), Renata Libonati (UFRJ)

New key indicator: Earth's energy imbalance – Karina von Schuckmann (Mercator Ocean international), Audrey Minière (ENS, LMD), Flora Gues (CELAD)

Climate and heat impacts on health – Joy Shumake-Guillemot (WMO), Petra Hongell (WMO), Sarah Holmes (WMO), Hunter Jones (WMO), Armel Castellan (WMO), Maddie West (WMO)

Reviewers

Abdulkarim A. Al-Maashi (NCM, Saudi Arabia), Mazen I. Asiri (NCM, Saudi Arabia), Lauriane Batte (Météo-France), Christine Berne (Météo-France), Véronique Bouchet (WMO), Sylvie Castonguay (WMO), Chun Wing Choy (Hong Kong Observatory), Robert Dunn (Met Office Hadley Centre), Awatif Ebrahim (Egyptian Meteorological Authority), Glauber Ferreira (INMET), Ana Morata Gasca (AEMET), Ana Heureux (WMO), Alejandro Jair García Jiménez (Servicio Meteorológico Nacional, Mexico), Andries Kruger (South African Weather Service), Sari Lappi (WMO), Renata Libonati (UFRJ), Jochen Luther (WMO), Sulagna Mishra (WMO), Colin Morice (Met Office Hadley Centre), Patricia Nying'uro (KMD), Hindumathi Palanisamy (WMO), Caroline Sandford (Met Office Hadley Centre), Serhat Sensoy (TSMS), Zablon Shilenje (WMO), Peter Siegmund (KNMI), Michael Sparrow (WMO), Barbara Tapia Cortes (WMO), Blair Trewin (BOM), Freja Vamborg (ECMWF), Narelle Van Der Wel (WMO), wAn Willems (RMI), Ken Yamada (JMA), Arjan O. Zamreeg (NCM, Saudi Arabia)

WMO programme coordination

Claire Ransom (Associate Scientific Officer), Peer Hechler (Scientific Officer), Sarah Holmes (UK Met Office/WMO), Byungjun Kim (WMO)

Endnotes

1. World Meteorological Organization (WMO). ***WMO Greenhouse Gas Bulletin, No. 21: The State of Greenhouse Gases in the Atmosphere Based on Global Observations through 2024;*** WMO: Geneva, 2025.
2. Montzka, S. A. *The NOAA Annual Greenhouse Gas Index (AGGI)*; National Oceanic and Atmospheric Administration (NOAA) Earth System Research Laboratories Global Monitoring Laboratory, 2024. http://www.esrl.noaa.gov/gmd/aggi/aggi.html.
3. Intergovernmental Panel on Climate Change (IPCC). *Climate Change 2021: The Physical Science Basis. Contribution of Working Group I to the Sixth Assessment Report of the Intergovernmental Panel on Climate Change*; Masson-Delmotte, V.; Zhai, P.; Pirani, A. et al., Eds.; Cambridge University Press: Cambridge, UK and New York, USA, 2021. https://doi.org/10.1017/9781009157896.
4. Friedlingstein, P.; O'Sullivan, M.; Jones, M. W. et al. Global Carbon Budget 2025. *Earth System Science Data* **2025** [preprint]. https://doi.org/10.5194/essd-2025-659.
5. Pan, Y.; Cheng, L.; Abraham, J. et al. Ocean Heat Content Sets Another Record in 2025. *Advances in Atmospheric Sciences* **2026**. https://doi.org/10.1007/s00376-026-5876-0.
6. Intergovernmental Panel on Climate Change (IPCC). Climate C hange 2021: *The Physical Science Basis. Contribution of Working Group I to the Sixth Assessment Report of the Intergovernmental Panel on Climate Change;* Masson-Delmotte, V.; Zhai, P.; Pirani, A. et al., Eds.; Cambridge University Press: Cambridge, UK and New York, USA, 2021. https://doi.org/10.1017/9781009157896.
7. An update of Johnson, G. C.; Purkey, S. G. Refined Estimates of Global Ocean Deep and Abyssal Decadal Warming Trends. *Geophysical Research Letters* **2024**, *51*. https://doi.org/10.1029/2024GL111229.
8. von Schuckmann, K.; Minière, A.; Gues, F. et al. Heat Stored in the Earth System 1960–2020: Where Does the Energy Go? *Earth System Science Data* **2023**, *15 (4)*, 1675–1709. https://doi.org/10.1029/2012GL051106.
9. Levitus, S.; Antonov, J. I.; Boyer, T. P. et al. World Ocean Heat Content and Thermosteric Sea Level Change (0–2 000 m), 1955–2010. *Geophysical Research Letters* **2012**, *39 (10)*. https://doi.org/10.1029/2012GL051106.
10. Cheng, L.; von Schuckmann, K.; Abraham, J. P. et al. Past and Future Ocean Warming. *Nature Reviews Earth & Environment* **2022**, 3, 776–794. https://doi.org/10.1038/s43017-022-00345-1.
11. Intergovernmental Panel on Climate Change (IPCC). *Climate Change 2021: The Physical Science Basis. Contribution of Working Group I to the Sixth Assessment Report of the Intergovernmental Panel on Climate Change;* Masson-Delmotte, V.; Zhai, P.; Pirani, A. et al., Eds.; Cambridge University Press: Cambridge, UK and New York, USA, 2021. https://doi.org/10.1017/9781009157896.
12. Intergovernmental Panel on Climate Change (IPCC). *IPCC Special Report on the Ocean and Cryosphere in a Changing Climate;* Pörtner, H.-O.; Roberts, D. C.; Masson-Delmotte, V. et al., Eds.; Cambridge University Press: Cambridge, UK and New York, USA, 2019. https://doi.org/10.1017/9781009157964.
13. https://wmo.int/el-ninola-nina-updates
14. Leclercq, L.; Oelsmann, J.; Cazenave, A. et al. Abrupt Trend Change in Global Mean Sea Level and Its Components in the Early 2010s. *Communications Earth and Environment* **2026**, 7. https://doi.org/10.1038/s43247-025-03149-5.
15. Intergovernmental Panel on Climate Change (IPCC). *Climate Change 2022: Impacts, Adaptation and Vulnerability. Contribution of Working Group II to the Sixth Assessment Report of the Intergovernmental Panel on Climate Change;* Pörtner, H.-O.; Roberts, D. C.; Tignor, M. et al., Eds.; Cambridge University Press: Cambridge, UK and New York, USA, 2022. https://doi.org/10.1017/9781009325844.
16. Gulev, S. K.; Thorne, P. W.; Ahn, J. et al. Changing State of the Climate System. In Climate Change 2021: *The Physical Science Basis. Contribution of Working Group I to the Sixth Assessment Report of the Intergovernmental Panel on Climate Change;* Masson-Delmotte, V.; Zhai, P.; Pirani, A. et al., Eds.; Cambridge University Press: Cambridge, UK and New York, USA, 2021. https://doi.org/10.1017/9781009157896.
17. von Schuckmann, K.; Moreira, L.; Cancet, M. et al. The State of the Global Ocean. In: *Copernicus Ocean State Report*, 8th edition; von Schuckmann, K.; Moreira, L.; Grégoire, M. et al., Eds.; Copernicus Publications, 2024. https://doi.org/10.5194/sp-4-osr8-1-2024.
18. Friedlingstein, P.; O'Sullivan, M.; Jones, M. W. et al. Global Carbon Budget 2025. *Earth System Science Data* **2025.** [preprint]. https://doi.org/10.5194/essd-2025-659.
19. Arias, P. A.; Bellouin, N.; Coppola, E. et al. Technical Summary. In Climate Change 2021: *The Physical Science Basis. Contribution of Working Group I to the Sixth Assessment Report of the Intergovernmental Panel on Climate Change;* Masson-Delmotte, V.; Zhai, P.; Pirani, A. et al., Eds.; Cambridge University Press: Cambridge, UK and New York, USA, 2021. https://doi.org/10.1017/9781009157896.

20. Landschützer, P.; Laruelle, G. G.; Roobaert, A. et al. A Uniform pCO2 Climatology Combining Open and Coastal Oceans. *Earth System Science Data* **2020**, *12*, 2537–2553. https://doi.org/10.5194/essd-12-2537-2020. Chau, T. T. T.; Gehlen, M.; Chevallier, F. A Seamless Ensemble-based Reconstruction of Surface Ocean pCO_2 and Air–Sea CO_2 Fluxes over the Global Coastal and Open Oceans. *Biogeosciences* **2022**, *19*, 1087–1109. https://doi.org/10.5194/bg-19-1087-2022.

21. Cooley, S.; Schoeman, D.; Bopp, L. et al. Oceans and Coastal Ecosystems and Their Services. In *Climate Change 2022: Impacts, Adaptation, and Vulnerability. Contribution of Working Group II to the Sixth Assessment Report of the Intergovernmental Panel on Climate Change;* Pörtner, H.-O.; Roberts, D. C.; Tignor, M. et al., Eds.; Cambridge University Press: Cambridge, UK and New York, USA, 2022. https://doi.org/10.1017/9781009325844.

22. Arias, P. A.; Bellouin, N.; Coppola, E. et al. Technical Summary. In *Climate Change 2021: The Physical Science Basis. Contribution of Working Group I to the Sixth Assessment Report of the Intergovernmental Panel on Climate Change;* Masson-Delmotte, V.; Zhai, P.; Pirani, A. et al., Eds.; Cambridge University Press: Cambridge, UK and New York, USA, 2021. https://doi.org/10.1017/9781009157896.

23. Intergovernmental Panel on Climate Change (IPCC). Summary for Policymakers. In: *Climate Change 2021: The Physical Science Basis. Contribution of Working Group I to the Sixth Assessment Report of the Intergovernmental Panel on Climate Change;* Masson-Delmotte, V.; Zhai, P.; Pirani, A. et al., Eds.; Cambridge University Press: Cambridge, UK and New York, USA, 2021. https://doi.org/10.1017/9781009157896.001.

24. Bindoff, N. L.; Cheung, W. W. L.; Kairo, J. G. et al. Changing Ocean, Marine Ecosystems, and Dependent Communities. In: *IPCC Special Report on the Ocean and Cryosphere in a Changing Climate;* Pörtner, H.-O.; Roberts, D. C.; Masson-Delmotte, V. et al., Eds.; Cambridge University Press: Cambridge, UK and New York, USA, 2019. https://doi.org/10.1017/9781009157964.007.

25. Intergovernmental Panel on Climate Change (IPCC). Summary for Policymakers. In *Climate Change 2022: Impacts, Adaptation, and Vulnerability. Contribution of Working Group II to the Sixth Assessment Report of the Intergovernmental Panel on Climate Change;* Pörtner, H.-O.; Roberts, D. C.; Tignor, M. et al., Eds.; Cambridge University Press: Cambridge, UK and New York, USA, 2022. https://doi.org/10.1017/9781009325844.001.

26. Intergovernmental Panel on Climate Change (IPCC). Summary for Policymakers. In *IPCC Special Report on the Ocean and Cryosphere in a Changing Climate;* Pörtner, H.-O.; Roberts, D. C.; Masson-Delmotte, V. et al., Eds.; Cambridge University Press: Cambridge, UK and New York, USA, 2019. https://doi.org/10.1017/9781009157964.001.

27. WCRP Global Sea Level Budget Group. Global Sea-level Budget 1993–Present. *Earth System Science Data* **2018**, *10*, 1551–1590. https://doi.org/10.5194/essd-10-1551-2018.

28. Intergovernmental Panel on Climate Change (IPCC). Summary for Policymakers. In: *Climate Change 2021: The Physical Science Basis. Contribution of Working Group I to the Sixth Assessment Report of the Intergovernmental Panel on Climate Change;* Masson-Delmotte, V.; Zhai, P.; Pirani, A. et al., Eds.; Cambridge University Press: Cambridge, UK and New York, USA, 2021. https://doi.org/10.1017/9781009157896.001.

29. Purich, A.; Doddridge, E. W. Record Low Antarctic Sea Ice Coverage Indicates a New Sea Ice State. *Communications Earth & Environment* **2023**. 4 (1). https://doi.org/10.1038/s43247-023-00961-9.

30. Intergovernmental Panel on Climate Change (IPCC). *Climate Change 2021: The Physical Science Basis. Contribution of Working Group I to the Sixth Assessment Report of the Intergovernmental Panel on Climate Change;* Masson-Delmotte, V.; Zhai, P.; Pirani, A. et al., Eds; Cambridge University Press: Cambridge, UK and New York, USA, 2021. https://doi.org/10.1017/9781009157896.

31. Cuesta-Valero, F. J.; Garcia-Garcia, A.; Beltrami, H. et al. Robust Increase in Observed Heat Storage by the Global Subsurface. *Science Advances* **2025**, *11*. https://doi.org/10.1126/sciadv.adw9958.

32. Minière, A.; von Schuckmann, K.; Sallée, J.-B. et al. Robust Acceleration of Earth System Heating Observed over the Past Six Decades. *Scientific Reports* **2023**, *13*. https://doi.org/10.1038/s41598-023-49353-1.

33. Storto, A.; Yang, C. Acceleration of the Ocean Warming from 1961 to 2022 Unveiled by Large-ensemble Reanalyses. *Nature Communications* **2024**, *15*, 545. https://doi.org/10.1038/s41467-024-44749-7.

34. Hansen, J.; Sato, M.; Kharecha, P. et al. Earth's Energy Imbalance and Implications. *Atmospheric Chemistry and Physics* **2011**, *11*, 13421–13449. https://doi.org/10.5194/acp-11-13421-2011.

35. Hansen, J. E.; Sato, M.; Simons, L. et al. Global Warming in the Pipeline. *Oxford Open Climate Change* **2023**, *3* (1). https://doi.org/10.1093/oxfclm/kgad008.

36. Global Climate Observing System (GCOS). ***The 2022 GCOS Implementation Plan*** (GCOS-244; Global Ocean Observing System (GOOS)-272); World Meteorological Organization (WMO): Geneva, 2022.

37. von Schuckmann, K.; Minière, A.; Gues, F. et al. Heat Stored in the Earth System 1960–2020: Where Does the Energy Go? *Earth System Science Data* **2023**, *15*, 1675–1709. https://doi.org/10.5194/essd-15-1675-2023.

38. Forster, P. M.; Smith, C.; Walsh, T. et al. Indicators of Global Climate Change 2024: Annual Update of Key Indicators of the State of the Climate System and Human Influence. *Earth System Science Data* **2025**, *17*, 2641–2680. https://doi.org/10.5194/essd-17-2641-2025.

39. Loeb, N. G.; Ham, S. H.; Allan, R. P. et al. Observational Assessment of Changes in Earth's Energy Imbalance Since 2000. *Surveys in Geophysics* **2024**, *45*, 1757–1783. https://doi.org/10.1007/s10712-024-09838-8.

40. Forster, P. T.; Storelvmo, T.; Armour, K. et al. The Earth's Energy Budget, Climate Feedbacks and Climate Sensitivity. In *Climate Change 2021: The Physical Science Basis. Contribution of Working Group I to the Sixth Assessment Report of the Intergovernmental Panel on Climate Change;* Masson-Delmotte, V.; Zhai, P.; Pirani, A. et al., Eds.; Cambridge University Press: Cambridge, UK and New York, USA, 2021. https://doi.org/10.1017/9781009157896.

41. Mauritsen, T.; Tsushima, Y.; Meyssignac, B. et al. Earth's Energy Imbalance More than Doubled in Recent Decades. *AGU Advances* **2025**, *6*. https://doi.org/10.1029/2024AV001636.

42. Forster, P. M.; Smith, C.; Walsh, T. et al. Indicators of Global Climate Change 2024: Annual Update of Key Indicators of the State of the Climate System and Human Influence. *Earth System Science Data* **2025**, *17*, 2641–2680. https://doi.org/10.5194/essd-17-2641-2025.

43. von Schuckmann, K.; Cheng, L.; Palmer, M. D. et al. Heat Stored in the Earth System: Where Does the Energy Go? *Earth System Science Data* **2020**, *12*, 2013–2041. https://doi.org/10.5194/essd-12-2013-2020.

44. von Schuckmann, K.; Minière, A.; Gues, F. et al. GCOS EHI 1960–2020 *Earth Heat Inventory Ocean Heat Content (Version 2);* World Data Center for Climate [dataset], 2023. https://doi.org/10.26050/WDCC/GCOS_EHI_1960-2020_OHC_v2.

45. Loeb, N. G.; Johnson, G. C.; Thorsen, T. J. et al. Satellite and Ocean Data Reveal Marked Increase in Earth's Heating Rate. *Geophysical Research Letters* **2021**, *48*. https://doi.org/10.1029/2021GL093047.

46. Raghuraman, S. P.; Paynter, D.; Ramaswamy, V. Anthropogenic Forcing and Response Yield Observed Positive Trend in Earth's Energy Imbalance. *Nature Communications* **2021**, *12*, 4577. https://doi.org/10.1038/s41467-021-24544-4.

47. Kramer, R. J.; He, H.; Soden, B. J. et al. Observational Evidence of Increasing Global Radiative Forcing. *Geophysical Research Letters* **2021**, *48*. https://doi.org/10.1029/2020GL091585.

48. Hansen, J. E.; Sato, M.; Simons, L. et al. Global Warming in the Pipeline. *Oxford Open Climate Change* **2023**, *3* (1). https://doi.org/10.1093/oxfclm/kgad008.

49. Goessling, H. F.; Rackow, T.; Jung, T. Recent Global Temperature Surge Intensified by Record-low Planetary Albedo. *Science* **2025**, *387*, 68–73. https://doi.org/10.1126/science.adq7280.

50. Allan, R. P.; Merchant. C. J. Reconciling Earth's Growing Energy Imbalance with Ocean Warming. *Environmental Research Letters* **2025**, *20*. DOI: 10.1088/1748-9326/adb448; Cuesta-Valero, F. J.; Garcia-Garcia, A.; Beltrami, H. et al. Robust Increase in Observed Heat Storage by the Global Subsurface. *Science Advances* **2025**, *11*. https://doi.org/10.1126/sciadv.adw9958.

51. World Meteorological Organization (WMO). ***El Niño/La Niña Update: February 2025***; WMO: Geneva, 2025.

52. Zheng, Y.; Hoteit, I. Asymmetric Impacts of Indian Ocean Dipole on Summer Climate over Arabian Peninsula. *Geophysical Research Letters* **2025**, *52*. https://doi.org/10.1029/2025GL118195.

53. https://internal.imd.gov.in/press_release/20250930_pr_4343.pdf

54. Intergovernmental Panel on Climate Change (IPCC). *AR6 Synthesis Report Headline Statements.* https://www.ipcc.ch/report/ar6/syr/resources/spm-headline-statements/.

55. FAO, IFAD, UNICEF, WFP, WHO. 2025. *The State of Food Security and Nutrition in the World 2025*; Rome, 2025. https://doi.org/10.4060/cd6008en.

56. Mehrabi, Z.; Delzeit, R.; Ignaciuk, A. et al. Research Priorities for Global Food Security under Extreme Events. *One Earth* **2022**, *5* (7), 756–766. https://pmc.ncbi.nlm.nih.gov/articles/PMC9307291/.

57. Intergovernmental Panel on Climate Change (IPCC). *Climate Change 2022: Impacts, Adaptation, and Vulnerability. Contribution of Working Group II to the Sixth Assessment Report of the Intergovernmental Panel on Climate Change;* Pörtner, H.-O.; Roberts, D. C.; Tignor, M., Eds.; Cambridge University Press: Cambridge, UK and New York, USA, 2022. https://doi.org/10.1017/9781009325844.

58. Internal Displacement Monitoring Centre (IDMC). *2025 Global Report on Internal Displacement.* IDMC, 2025. https://doi.org/10.55363/IDMC.XTGW2833.

59. I. https://www.ncei.noaa.gov/access/monitoring/monthly-report/national/202507

    II. https://www.fire.ca.gov/incidents/2025/1/7/palisades-fire; https://www.fire.ca.gov/incidents/2025/1/7/eaton-fire

    III. CalFire incident reports, https://www.fire.ca.gov/incidents/2025

    IV. EM-DAT International Disaster Database

    V. Kelley, D. I.; Burton, C.; Di Giuseppe, F. et al. State of Wildfires 2024–2025. *Earth System Science Data* **2025**, *17*, 5377–5488. https://doi.org/10.5194/essd-17-5377-2025.

VI. Internal Displacement Monitoring Centre (IDMC), 2025: internal-displacement.org; https://www.internal-displacement.org/expert-analysis/wildfire-displacement-is-on-the-rise-2025-sends-a-clear-warning/.

VII. https://forest-fire.emergency.copernicus.eu/apps/effis.statistics/estimates

VIII. EM-DAT; https://reliefweb.int/map/nigeria/nigeria-l-flood-impact-mokwa-town-dg-echo-daily-map-13062025.

IX. https://dtm.iom.int/reports/nigeria-joint-flood-situation-report-niger-state-02-june-2025?close=true; https://www.aljazeera.com/news/2025/6/1/nigeria-flash-floods-which-is-most-affected-area-what-caused-the-deluge

X. https://reliefweb.int/report/democratic-republic-congo/democratic-republic-congo-floods-ifrc-unosat-international-charter-mettelsat-echo-daily-flash-14-april-2025

XI. https://ndma.gov.pk/sitrepm; https://www.ndma.gov.pk/storage/sitreps/October2025/oztOSIiYIDcY1OCXxsBV.pdf

XII. https://reliefweb.int/report/pakistan/rapid-needs-assessment-assessing-scale-and-scope-impact-response-kp

XIII. IDMC, 2025: internal-displacement.org.

XIV. World Food Programme (WFP) Advanced Disaster Analysis and Mapping (ADAM) as of 11 Sept 2025: https://static.gis.wfp.org/adam_fl/event/20250918/ADAM_PAK_FloodReport_20250918.pdf

XV. https://reliefweb.int/report/bangladesh/iom-bangladesh-rohingya-humanitarian-crisis-response-situation-update-april-june-2025

XVI. Food and Agriculture Organization of the United Nations (FAO) Global Information and Early Warning System on Food and Agriculture (GIEWS), July 2025; https://www.fao.org/giews/countrybrief/country/IRN/pdf/IRN.pdf.

XVII. WFP ADAM: https://static.gis.wfp.org/adam_fl/event/20250124/ADAM_MOZ_FloodReport_20250124.pdf

XVIII. https://www.unhcr.org/sites/default/files/2025-02/Cyclone%20Chido%20Flash%20Appeal%20_%20Final%2020250131.pdf

XIX. https://dtm.iom.int/reports/mozambique-tropical-cyclone-jude-flash-update-2-24-march-2025

XX. https://reliefweb.int/report/mozambique/mozambique-multi-cluster-initial-rapid-assessment-mira-tropical-cyclone-jude-nampula

XXI. WFP ADAM: https://static.gis.wfp.org/adam_fl/event/20250318/ADAM_MOZ_FloodReport_20250318.pdf

XXII. https://www.unhcr.org/sites/default/files/2025-05/UNHCR%20Mozambique%20Operational%20Update%20%28Jan-Mar%202025%29%20_%20distribution.pdf

XXIII. South Africa contribution

XXIV. IDMC, 2025: https://www.internal-displacement.org/; see also South Africa contribution

XXV. Republic of Korea contribution

XXVI. https://www.gfdrr.org/en/JamaicaGRADE

XXVII. https://reliefweb.int/report/haiti/unicef-haiti-flash-update-no-3-hurricane-melissa-24-october-24-november-2025

XXVIII. https://reliefweb.int/report/jamaica/iom-caribbean-hurricane-melissa-situation-report-no-14-17-december-2025

XXIX. https://ndrrmc.gov.ph/wp-content/uploads/2025/11/Situational_Report_No._30_for_the_Effects_of_Tropical_Cyclone_TINO_2025.pdf

XXX. https://reliefweb.int/report/cambodia/philippines-viet-nam-laos-cambodia-tropical-cyclone-kalmaegi-update-gdacs-jtwc-pagasa-ndrrmc-echo-daily-flash-5-november-2025

XXXI. https://reliefweb.int/report/philippines/philippines-tropical-cyclones-kalmaegitino-and-fung-wonguwan-flash-update-no-2-11-november-11-pm-local-time

XXXII. https://www.un.org/en/delegate/how-anticipatory-action-shaped-response-philippines%E2%80%99-twin-typhoons

XXXIII. https://dromic.dswd.gov.ph/wp-content/uploads/2026/02/DSWD-DROMIC-Report-78-on-the-Effects-of-Super-Typhoon-Uwan-as-of-04-February-2026-6PM.pdf

XXXIV. IDMC, 2025: internal-displacement.org

XXXV. https://reliefweb.int/report/viet-nam/unicef-viet-nam-situation-report-no-01-typhoons-bualoi-and-matmo-north-and-central-viet-nam-reporting-date-10-october-15-october

XXXVI. https://reliefweb.int/report/viet-nam/viet-nam-central-flood-2025-dref-operation-mdrvn026

XXXVII. https://reliefweb.int/report/indonesia/indonesia-floods-and-landslides-update-bnpb-adinet-bmkg-echo-daily-flash-15-december-2025

XXXVIII. https://gis.bnpb.go.id/BANSORSUMATERA2025/

XXXIX. Economic loss data from EM-DAT

XL. https://reliefweb.int/report/thailand/thailand-malaysia-severe-weather-floods-and landslides-update-adinet-noaa-cpc-echo-daily-flash-12-december-2025

XLI. https://www.dmc.gov.lk/images/dmcreports/Situation_Report_at_1630hrs_on_2025__1765623695.pdf

60. Sophia, Y.; Roxy, M. K.; Murtugudde, R. et al. Dengue Dynamics, Predictions, and Future Increase Under Changing Monsoon Climate in India. *Scientific Reports* **2025**, *15*, 1637. https://doi.org/10.1038/s41598-025-85437-w.

61. Haider, N.; Hasan, M. N.; Onyango, J. Global Dengue Epidemic Worsens with Record 14 Million Cases and 9 000 Deaths Reported in 2024. *International Journal of Infectious Diseases* **2025**, *158*. https://doi.org/10.1016/j.ijid.2025.107940.

62. https://www.who.int/news-room/fact-sheets/detail/dengue-and-severe-dengue

63. https://www.who.int/news/item/22-08-2025-who-wmo-issue-new-report-and-guidance-to-protect-workers-from-increasing-heat-stress

64. WHO, WMO issue new report and guidance to protect workers from increasing heat stress https://www.who.int/news/item/22-08-2025-who-wmo-issue-new-report-and-guidance-to-protect-workers-from-increasing-heat-stress: World Meteorological Organization (WMO); World Health Organization (WHO). ***Climate Change and Workplace Heat Stress: Technical Report and Guidance***; WMO/WMO, 2025.

65. World Meteorological Organization (WMO). ***2023 State of Climate Services*** (WMO-No. 1335). Geneva, 2023.

66. https://www.who.int/initiatives/who-wmo-joint-climate-and-health-programme

67. Intergovernmental Panel on Climate Change (IPCC). Climate Change 2021: *The Physical Science Basis. Contribution of Working Group I to the Sixth Assessment Report of the Intergovernmental Panel on Climate Change;* Masson-Delmotte, V.; Zhai, P.; Pirani, A. et al., Eds.; Cambridge University Press: Cambridge, UK and New York, USA, 2021. https://doi.org/10.1017/9781009157896.

For more information please visit:
wmo.int/resources/publication-series

WORLD
METEOROLOGICAL
ORGANIZATION